Molecular Biology and Evolution, 2025, **42**, 1–19
https://doi.org/10.1093/molbev/msaf292
Advance access publication 15 December 2025
Discoveries

Coexisting With Humans: Genomic and Behavioral Consequences in a Small and Isolated Bear Population

Giulia Fabbri,[1,†] **Roberto Biello**,[1,†] **Maëva Gabrielli**,[1,2,†] **Sibelle Torres Vilaça**,[1,3] **Beatrice Sammarco**,[1] **Silvia Fuselli**,[1] **Patrícia Santos**,[1] **Lorena Ancona**,[4] **Laura Peretto**,[1] **Giada Padovani**,[1,5] **Marco Sollitto**,[6,7] **Alessio Iannucci**,[8] **Ladislav Paule**,[9] **Dario Balestra**,[1] **Marco Gerdol**,[6] **Claudio Ciofi**,[8] **Paolo Ciucci**,[10] **Carolyn G. Mahan**,[11] **Emiliano Trucchi**,[4] **Andrea Benazzo**,[1,*†] **Giorgio Bertorelle**[1]

[1]Department of Life Sciences and Biotechnologies, University of Ferrara, Ferrara, Italy
[2]Centre de Recherche sur la Biodiversité et L'Environnement (CRBE), Université de Toulouse, CNRS, IRD, Toulouse INP, Toulouse, France
[3]Vale Institute of Technology, Belém, Brazil
[4]Department of Life and Environmental Sciences, Marche Polytechnic University, Ancona, Italy
[5]Department of Environmental Engineering Sciences, University of Florida, Gainesville, FL, USA
[6]Department of Life Sciences, University of Trieste, Trieste, Italy
[7]The Vertebrate Genome Laboratory, The Rockefeller University, New York City, NY, USA
[8]Department of Biology, University of Florence, Firenze, Italy
[9]Department of Phytology, Technical University in Zvolen, Zvolen, Slovakia
[10]Department of Biology and Biotechnologies, Sapienza University of Rome, Roma, Italy
[11]Department of Biology, Penn State University, Altoona, PA, USA

[†]These authors contributed equally.
***Corresponding author:** Email: andrea.benazzo@unife.it.
Associate editor: Joanna Kelley

Abstract

Climate and land use change have increased human–wildlife interactions, potentially reducing wild species density and prompting behavioral adaptations to urbanized environments. It is still debated if behavioral responses are mainly the result of phenotypic plasticity or if they were driven by anthropic selective pressures, especially in small populations where genetic drift is strong. Our study focused on the small Apennine brown bear population (*Ursus arctos marsicanus*), which has coexisted with humans in Central Italy for millennia. We characterized genomic diversity and identified adaptation signals distinctive to this population by comparing newly generated and published whole-genome resequencing data from Apennine, Central European, and North American brown bears. Apennine brown bears exhibited reduced genomic diversity, higher inbreeding, and larger realized genetic load compared to other brown bears. We showed that Apennine brown bears possess a unique genomic diversity pattern including selective signatures at genes associated with reduced aggressiveness (eg *DCC*, *SLC13A5*). Within these genes, most of the newly discovered variants were located in noncoding regions and some of them were predicted to alter splicing factor binding sites, highlighting the contribution of noncoding variation in shaping complex phenotypes. Our results support the hypothesis that human-induced selection has promoted behavioral changes even in small- and long-isolated populations, reducing conflicts and contributing to the long-term persistence of a large mammal species and its coexistence with humans.

Keywords: conservation genomics, selection, genetic load, comparative genomics, genomic monitoring, *Ursus arctos marsicanus*, aggressiveness

Introduction

Humans have long influenced the environment in which they lived and thrive, affecting ecosystems and biodiversity (Palumbi 2001; Otto 2018). Habitat change and overexploitation are among the human activities with the greatest impacts on vertebrate taxa (Pelletier and Coltman 2018), and can result in population decline and reduced gene flow, ultimately modifying the evolutionary trajectory of species (Allendorf and Hard 2009; Ripple et al. 2014; Pelletier and Coltman 2018). While animals may initially respond to selective pressures with plastic behavioral adaptations, persistent pressure can drive evolutionary adaptation through genetically based behavioral modifications (Tuomainen and Candolin 2011). This process drives a population-wide, coherent shift in a series of correlated reaction norms to better align with the environment (Sih et al. 2004). Indeed, wildlife can respond to anthropogenic disturbance by adjusting its behavior to facilitate the coexistence with humans via human avoidance, limited dispersion, habituation—the learning process by which an animal comes to perceive the human presence as neutral—and possibly less aggressive behavior (Whittaker and Knight 1998; McDougall et al. 2006; Oriol-Cotterill et al. 2015; Schell et al. 2021), which has an hereditary component (Trut 1999).

The study of the ecology of animals living in human-dominated landscapes has already produced a substantial

Received: June 10, 2025. **Revised:** October 8, 2025. **Accepted:** October 23, 2025

body of knowledge (Tuomainen and Candolin 2011; Donihue and Lambert 2015; Mancinelli et al. 2019; Beckman et al. 2022), with many reports of behavioral changes (Breck et al. 2019; Lewis et al. 2021; Brown et al. 2023). For example, Martínez-Abraín et al. (2019) hypothesized that the prolonged human persecution of several bird and mammal species led to the survival of the shy and less exploratory individuals in a population. However, few studies have linked such altered phenotypes to a genetic base (eg Mueller et al. 2013). One great challenge remains to understand the relative roles of phenotypic plasticity and adaptive evolution in response to anthropogenic disturbance in a rapidly changing world (Charmantier and Gienapp 2014; Merilä and Hendry 2014; Levis and Pfennig 2020).

The Apennine brown bear (henceforth called ABB), *Ursus arctos marsicanus*, is a small, endemic and isolated bear population found only in Central Italy, with a long evolutionary history of coexistence with humans. Previous studies using resequenced whole genome data showed that this population diverged from other European brown bears 2,000 to 3,000 years ago and have remained completely isolated for at least the past ~1,500 years (Benazzo et al. 2017). One of the main factors promoting its isolation was forest clearance and land cover change related to spread of agriculture and increasing human density in Central Italy. Human persecution has been well documented since Roman times (Epplett 2001), aimed at controlling bear density and expanding urbanized areas (Jennison 1937; Albrecht et al. 2017).

The present ABB population of approximately 50 individuals (Ciucci et al. 2015) shows phenotypic differences from other brown bear populations, such as smaller body size, unique cranial morphology (Loy et al. 2008; Colangelo et al. 2012; Meloro et al. 2017), and less aggressive behavior (Benazzo et al. 2017; Thompson 2018) compared with European, North American, and Asian populations (Penteriani et al. 2016; Bombieri et al. 2021). Despite the overall low genomic variation and high levels of inbreeding, Benazzo et al. (2017) showed that high variation was maintained at key loci for survival. This suggests that natural selection might have contributed to shaping the genetic diversity of ABB particularly in cases where adaptation is of critical importance. Interestingly, Benazzo et al. (2017) also found that a pool of genes frequently associated with aggressiveness or tameness in other species was collectively enriched for fixed alternative alleles in ABB, suggesting that behavioral differences with other brown bear populations might be genetically determined. Whether directional selection induced by human persecution targeting more aggressive animals or genetic drift drove this differentiation remains an open question.

Here we focused on the recent evolutionary changes produced by human activities in this isolated and endangered group of bears. We generated a new high-quality chromosome-level reference genome for the ABB and resequenced 20 whole genomes of the ABB and bears from a larger European population in Slovakia (SBB), used here for comparison together with published genomes of American brown bears. Population genomic analyses were used to characterize the demographic and selective patterns, with a special focus on the genomic signatures of directional selection in the ABB population. Our findings suggest that selection on genetic variants related to behavior, likely driven by the human removal of more aggressive individuals, favored the emergence of a much less aggressive bear population and a less conflictual coexistence between humans and bears.

Results

Chromosome-Level Genome Assembly of the Apennine Brown Bear

Considering the isolation of the ABB from all the other brown bear populations and subspecies, and its unique genetic and phenotypic characteristics, we first assembled an ABB reference genome. We generated 91 Gb of PacBio long reads and 74.3 Gb of Illumina reads for the chromatin conformation capture (Hi-C) library, corresponding to a sequencing depth of approximately 40× and 34×, respectively. Combining PacBio and Hi-C data, we obtained a primary genome assembly (including the mitochondrial sequence) spanning 2.28 Gb organized in 371 scaffolds, with an N50 of 71.43 Mb and an L50 of 13, in agreement with the genome size estimation from kmers (Figure S1) and the grizzly bear genome assembly (Armstrong et al. 2022). The Hi-C contact matrix supported the presence of 37 scaffolds constituting 99.45% of the assembly (Figure S2), concordant with the known karyotype of the sequenced female (36 autosomes and the X chromosome) (Figure S3). Metrics computed on the final assembled genome suggested a high completeness for the genic and nongenic part of the genome and a low amount of nucleotide errors (Table S1). The scaffold lengths and their chromosome-scale relationships to the *U. arctos* assembly (Armstrong et al. 2022) are summarized in Table S2.

A total of 22,608 protein-coding genes were predicted and functionally annotated in the ABB genome, showing high completeness metrics, similar to those observed in the grizzly and polar bear genomes (Table S3).

When compared with other carnivora species, the ABB genome, included within the brown bear clade in the Ursidae family, confirmed the high synteny levels of all brown bears (Corbo et al. 2022) while also revealing some chromosomal rearrangements (Fig. 1 and Figure S4). In particular, scanning the ABB genome at a fine scale, we identified a 7.3-Mb chromosomal inversion containing the major histocompatibility complex (MHC) locus, located at one end of scaffold 31 (Fig. 1). The synteny analysis also highlighted that the same genomic region containing several MHC genes was translocated in the polar bear genome but with a different orientation than the ABB genome. Using a combination of targeted PCR amplification using newly designed primers and long-read mapping, we validated the inversion in four ABB samples, two SBB samples, and one sample from the Italian Alps.

Human-Driven Genomic Erosion in the Apennine Brown Bear

Thirteen high-coverage whole-genome resequencing data from ABB individuals—12 from this study and one from Benazzo et al. (2017)—were analyzed alongside nine SBB genomes—eight from this study and one from Benazzo et al. (2017)—as representatives of the western Eurasian clade of European brown bears (Davison et al. 2011; de Jong et al. 2023). Additional genomes from other European bears, available in GenBank (Table S4), were used in some analyses, although their sample sizes per population were very limited. Using a multi-reference alignment pipeline, we retrieved 12 million biallelic single-nucleotide polymorphisms (SNPs) in the whole dataset, with 2,196,467 and 7,016,199 variants segregating in the ABB and SBB populations, respectively (Table S5).

Phylogenetic analysis of the brown bear populations across Europe confirmed that the ABB forms a distinct subclade within the brown bear clade (Benazzo et al. 2017). This subclade is

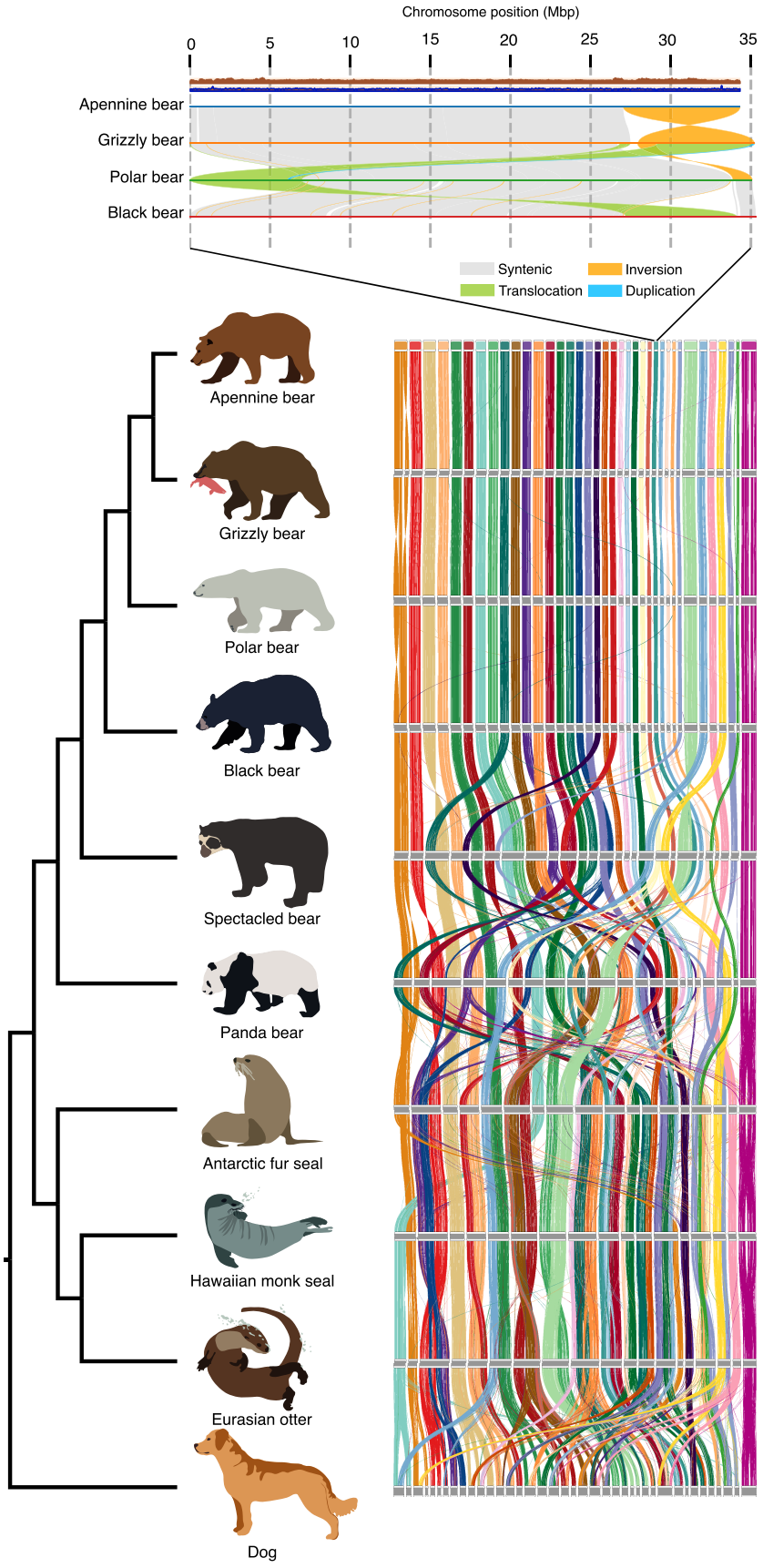

Fig. 1. Patterns of chromosome synteny within Carnivora. Pairwise macrosynteny based on 9,054 single-copy BUSCO genes. Color codes are based on ABB scaffold/chromosome organization. Chromosome alignment between *Ursus* species depicting the MHC inversion between Apennine and grizzly bears is shown on top. Coverage variations along the scaffold for Illumina and PacBio reads are also shown in brown and blue tracks, respectively.

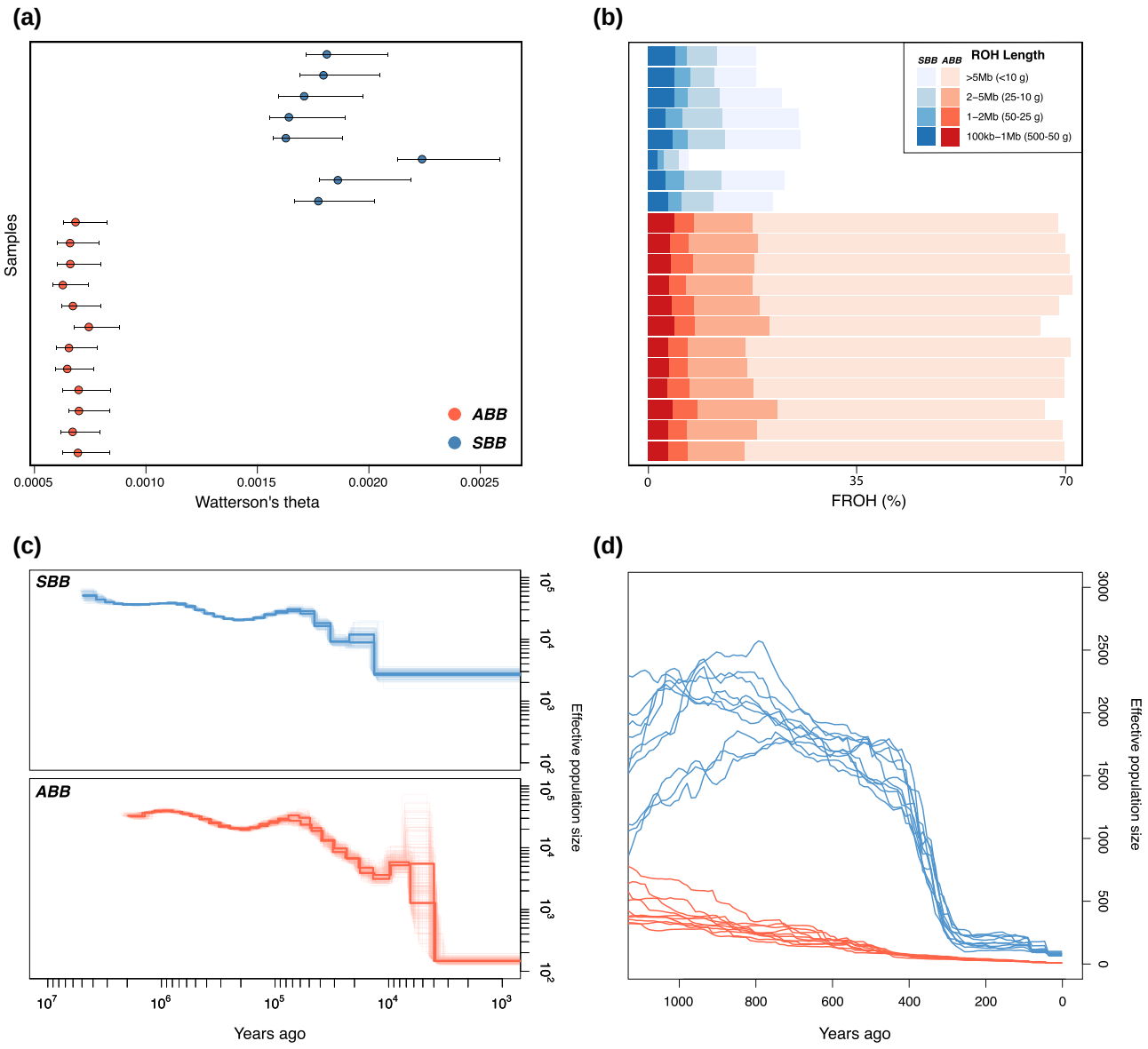

Fig. 2. Genomic diversity and demographic history of Apennine brown bears and Slovak brown bears. a) Genomic diversity estimates based on Watterson's Theta. b) Inbreeding coefficients (F_{ROH}) and corresponding time of inbreeding (generations before present) for each sample. The expected inbreeding time of a particular length of ROH was estimated using $g = 100/(2rL)$, where g is the expected generations that dates back to when both paternal and maternal lineages shared a common ancestor, r is the recombination rate, and L is the length of ROH. c) Past effective population size dynamics of ABB (8,657, 4,573, and 4,212 samples) and SBB (U1897, U1916, and U1919 samples) based on PSMC. The six genomes with the highest coverage for each population are shown. d) Recent effective population size dynamics analysis based on GONE. Ten independent replicates are shown.

characterized by short terminal branches (Figure S5), in agreement with the lower genomic diversity and higher inbreeding that we found in the ABB compared to other European brown bears (Figure S6a). In particular, all ABB individuals had a Watterson's theta lower than the one of any SBB individual (Fig. 2a). SBB had similar genetic variation to bears from all the other European areas, with the exception of brown bears from Spain showing an intermediate value (Figure S6a). Considering regions outside the runs of homozygosity (ROHs), levels of genetic diversity were similar among all European bears, suggesting that after excluding the high inbreeding levels in the ABB population (represented by ROH regions), ABB is as diverse as all European brown bears (Figure S6b).

The fraction of the genome in ROHs (F_{ROH}) was always higher than 66% in the ABB individuals, whereas in the SBB, this fraction ranged from 6.9% to 26% (Fig. 2b). Additionally, all ABB individuals exhibited a higher proportion of very long ROH segments (longer than 5 Mb), likely reflecting recent inbreeding events that occurred within the past ten generations.

As previously inferred from the analysis of a single individual (Benazzo et al. 2017), the Pairwise Sequentially Markovian Coalescent (PSMC) demographic reconstruction indicated a strong bottleneck in the ABB a few thousand years ago, which was not observed in the SBB (Fig. 2c). Interestingly, when the linkage disequilibrium pattern was used to infer the more recent demographic history over the last millennium, a strong but more recent bottleneck is suggested to occur in the SBB as well (Fig. 2d).

ABB showed fewer total derived genotypes predicted to be synonymous, mildly deleterious, or highly deleterious than SBB (Fig. 3a–c). In SBB, about one-third of the sites carrying these mutations were homozygous and two-thirds were

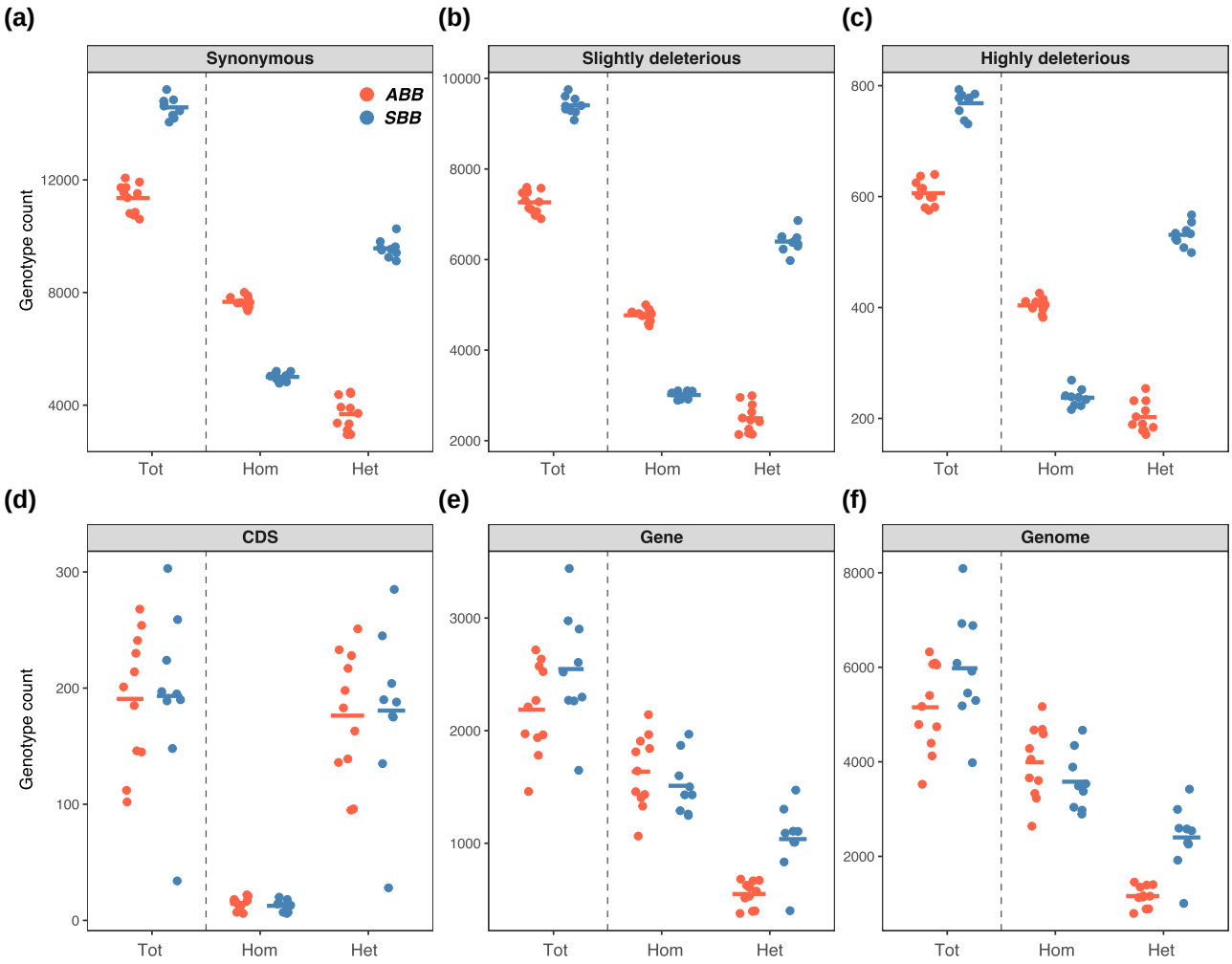

Fig. 3. Genetic load comparison of derived variants between ABB and SBB populations. a–c) represent SNP-based genetic load categorized as synonymous, slightly deleterious, and highly deleterious, respectively, classified into total (Tot), homozygous (Hom), and heterozygous (Het) variants. d–f) show the genetic load measured from the count of large deletions (structural variants between 50 bp and 10 Mb), in coding sequence (CDS), gene-level, and whole genome, respectively, classified into total (Tot), homozygous (Hom), and heterozygous (Het) variants. Horizontal bars indicate the mean of each group.

heterozygous. In contrast, the opposite pattern was observed in ABB.

The estimation of allele age for genome-wide deleterious variants showed that the age of a large fraction of slightly and highly deleterious mutations observed in the ABB population predates the ABB isolation from the European brown bear population (Figure S7).

We also identified high-quality genotyped deletions (DELs) for each individual of the ABB and SBB populations. The DELs were between 50 bp and 10 Mb long. The variation patterns in numbers of DELs across populations (ABB vs. SBB), genotypes (homozygote vs. heterozygote), and genomic regions (whole genomes vs. genes vs. coding sequences) are complex and probably affected by several biological and technical factors.

Firstly, the number of DELs observed in coding sequences (CDS) was similar in ABB and SBB individuals, considering the total number or partitioning it in homozygous and heterozygous genotypes (Fig. 3d; Mann–Whitney U test, P-value = 0.882, 0.445, and 0.882, respectively). Also, in both populations, the majority of DELs in CDS were found in the heterozygous state, with a very low number of homozygous genotypes (Fig. 3d).

Secondly, we found no statistically significant differences for ABB and SBB in the total amount of DELs per individual at the genomic and genic level (Mann–Whitney U test, P-value = 0.152 and 0.131, respectively) (Fig. 3e and f; Table S6). This pattern was mainly sustained by the derived homozygous DELs (P-value = 0.201 and 0.362). Nevertheless, heterozygous DELs were lower in ABB than SBB (P-value = 0.0008 at both the genic and genomic level), consistent with their lower genetic variability (Fig. 2a). Moreover, the average of the individual difference between the number of homozygous and heterozygous DELs at both the genic and genomic levels was higher in ABB compared to SBB, and this difference was statistically significant (P-value = 0.0001429 and 0.0003541).

Finally, assuming that gene connectivity, measured by the number of protein–protein interactions, serves as a proxy for the functional relevance of a gene (Chen et al. 2020; Liang et al. 2024), we also observed that in all the individuals, genes with DEL alleles in the CDS are, on average, less functionally relevant than genes with DEL alleles in introns (Mann–Whitney U test, P-value = 3.26×10^{-5}, Table S7).

Behavioral Shifts in a Human-Dominated Landscape

We applied different methods specifically designed to detect signatures of positive selection to the SNP dataset: Raised

Accuracy in Sweep Detection (RAiSD; Alachiotis and Pavlidis 2018), cross-population composite likelihood ratio (XP-CLR; Chen et al. 2010), and Population Branch Statistics (PBS; Yi et al. 2010). RAiSD summarizes multiple signatures of selective sweeps in the μ statistic, computed on a single population. XP-CLR compares allelic frequencies between pairs of populations. PBS was performed on four populations, with the ABB as the target. Only genes ranking in the top 1% in ABB and not displaying a similar outlier pattern in other populations or population pairs were selected (see Materials and Methods for details). A similar approach was applied to the structural variant (SV) datasets; however, only the PBS method was applicable. This first analysis identified a list of 566 genes under selection in the SNP dataset (Fig. 4 and Table S8) and 206 genes in the SV dataset (Table S9). Twenty genes were common to both lists.

To verify that the genes putatively under positive selection exhibited a different variation pattern than the rest of the genome, we computed Tajima's *D* statistics for various partitions of the SNP dataset (Figure S8). In both ABB and SBB, random genes and intergenic regions showed an average Tajima's *D* between 1.1 and 1.5, respectively. For the candidate genes under selection in ABB, however, the average Tajima's *D* was −0.03 in ABB and 1.2 in SBB.

Next, we performed Gene Ontology (GO) and human phenotype (HP) enrichment analyses to identify overrepresented functions and phenotypes in the lists of selected genes. Twenty GO terms were enriched in the SNP dataset (Table S10), and four in the SV dataset (Table S11). The former list included terms like developmental process (*P*-value = 0.0001) and biological regulation (*P*-value = 0.023), suggesting possible developmental and regulatory alterations in the ABB. Interestingly, five genes with known functions in the nervous system contributed to the enrichment of those terms: bromodomain PHD finger transcription factor (*BPTF*; Fitak et al. 2020), DCC netrin 1 receptor (*DCC*; Montague et al. 2014), G protein subunit alpha q (*GNAQ*; Pendleton et al. 2018), glutamate ionotropic receptor kainate type subunit 3 (*GRIK3*; Theofanopoulou et al. 2017), and glutamate metabotropic receptor 7 (*GRM7*; O'Rourke and Boeckx 2020).

The HP enrichment analysis identified nine statistically significant terms, all derived from the SNP dataset. Among these, the category "overfriendliness" included seven genes—BUD23 rRNA methyltransferase and ribosome maturation factor (*BUD23*), DnaJ heat shock protein family (Hsp40) member C30 (*DNAJC30*), methyltransferase like 27 (*METTL27*), SWI/SNF related BAF chromatin remodeling complex subunit ATPase 2 (*SMARCA2*), syntaxin 1A (*STX1A*), transmembrane protein 270 (*TMEM270*), VPS37D subunit of ESCRT-I (*VPS37D*)—six of which cluster in a chromosomal region deleted in human patients affected by the neurological disorder known as Williams–Beuren syndrome.

Finally, a manual screening of the selected gene list identified five additional outliers with roles in brain development: astrotactin 1 (*ASTN1*; Schubert et al. 2014), NUMB endocytic adaptor protein (*NUMB*; Schubert et al. 2014), gamma-aminobutyric acid type A receptor subunit beta2 (*GABRB2*; Fallahsharoudi et al. 2017), oxytocin receptor (*OXTR*; Fam et al. 2018; Herbeck et al. 2022), and solute carrier family 13 member 5 (*SLC13A5*; Hulsman Hanna et al. 2014; Rigby et al. 2022).

Therefore, we identified 17 genes putatively under selection with influence on the nervous system, or even more specifically that have been previously found to be associated with a complex behavior. The pattern of divergence between ABB and other brown bears at these genes revealed that the SNPs showing the largest differences in allelic frequencies were located outside the coding regions. Considering the potential phenotypic outcomes arising from the maturation of the same pre-RNA into alternative mature mRNA (Peng et al. 2017; Park et al. 2018; Zhou et al. 2021), we focused on genes in which intronic deletions and/or splicing anomalies may have contributed to the observed reduced aggressiveness that characterizes the ABB population. *DCC*, a transmembrane protein that intervenes in axon guidance during the formation of the nervous system, showed a substantial allele frequency difference between ABB and other bears at a SNP predicted to be a high-confidence splice-altering variant, leading to the loss of an acceptor site in intron 12 (delta score > 0.5 in SpliceAI analysis). Another gene of particular interest was *SLC13A5*, a sodium-dependent citrate cotransporter with crucial role in the regulation of metabolism and human brain development and functioning (Selch et al. 2018). The potential role of non-coding variants as behavioral modifiers in this gene was supported by the analysis of highly differentiated SNPs. A nearly fixed synonymous mutation in ABB (Scaffold_16:11681411) was linked to an exonic splicing silencer (ESS). Specifically, the ratio of ESS to exonic splicing enhancers was 5 in the sequence context of the major allele in ABB, while it was null for the minor allele according to HOT-SKIP analysis, suggesting that this variant could promote exon 6 skipping during mRNA splicing in ABB. Furthermore, this gene harbors one highly differentiated SNP that was predicted to create a donor splice site according to SpliceAI analysis, and ten highly differentiated SNPs that were predicted to change the motifs recognized by various splicing factors as suggested by the SpliceAid2 analysis (Table S12).

Discussion

Understanding how wild species respond to anthropogenic pressure over time is crucial for their preservation and successful coexistence with humans. In this study, both previously published and new whole-genome sequencing data were used to investigate the genomic impacts of anthropic pressure and isolation in the ABB, a small relict population of bears in Central Italy, where cohabitation with local human communities has been documented for several millennia.

Comparative genomics analysis based on a newly generated reference genome for the ABB indicates a shared genomic organization among European brown bears, which was not observed in the North American grizzly bear genome. This observation is in agreement with the genomic and mitochondrial differentiation observed between North American and European brown bears (de Jong et al. 2023). A noteworthy example was the genomic region containing the MHC locus characterized by high structural variation among the *Ursus* genus, suggesting that this fast-evolving region might play a key role in the process of species and population divergence (Eizaguirre et al. 2009). Therefore, European bears possess unique chromosomal features, highlighting the need for a distinct reference genome to better study the evolution of this species.

Our phylogenetic results confirm that the ABB forms a distinct genetic subclade within European brown bears, characterized by low genomic diversity and extensive inbreeding. The extremely high proportion of the genome in ROHs (>66%) and the prevalence of very long ROH segments in ABB indicate recent consanguineous mating, in contrast to

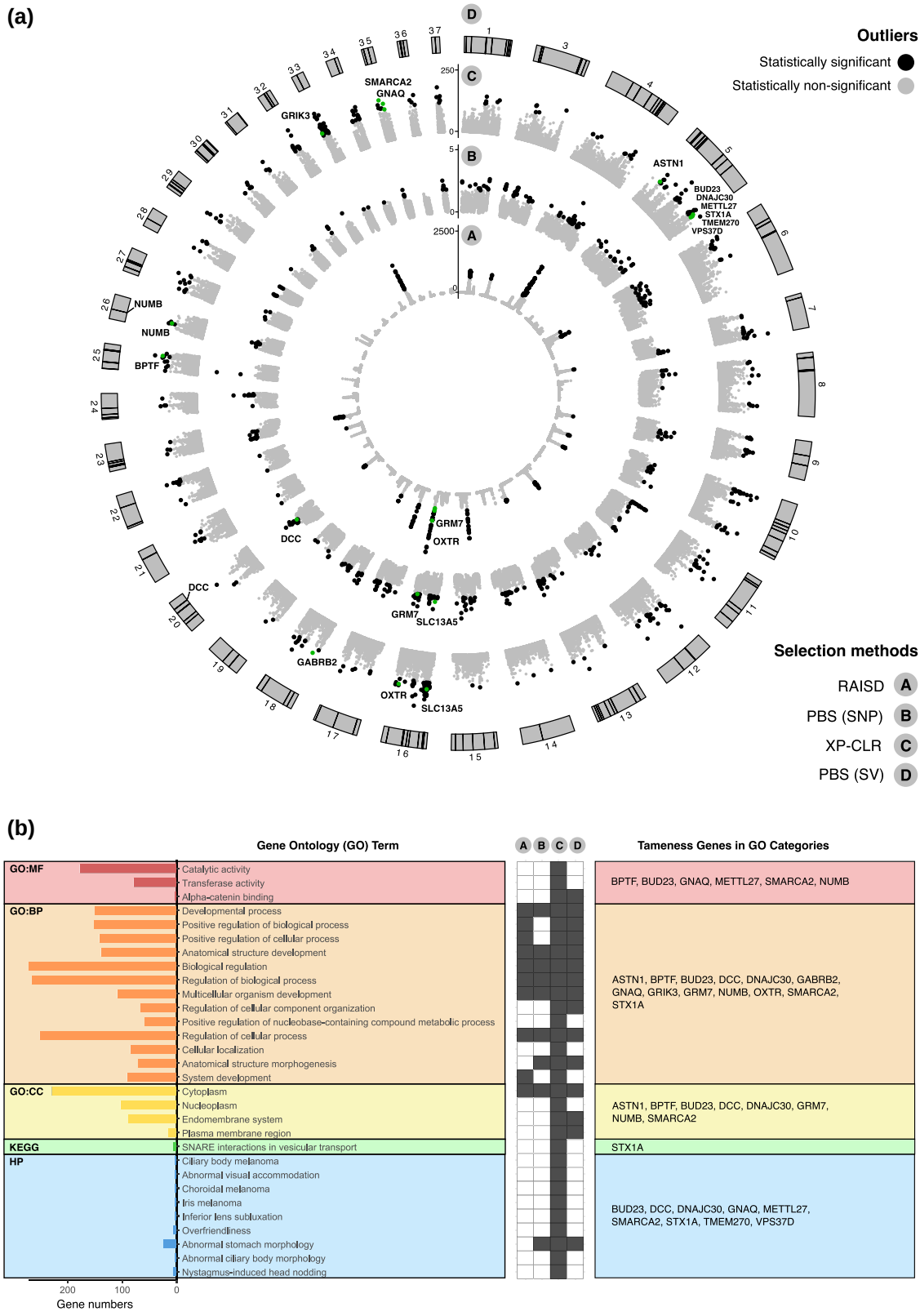

Fig. 4. Selection scans and enrichment analyses. a) Circos plots of the three selection scans performed on the SNPs dataset (RAiSD, XP-CLR, PBS-SNP) and the selection scan performed on the structural variants (SVs) dataset (PBS-SV) with the Apennine brown bear (ABB) as the target population. The threshold for defining outlier genomic windows or SVs was the top 1% of the distribution of values for each statistic (black dots). The 17 candidate genes that we identified as possibly determining a less aggressive behavior in ABB are reported close to their corresponding outlier window (in green). b) Enrichment analysis performed separately on the 566 outlier genes from the selection scans on the SNPs dataset and the 206 outlier genes from the selection scan on the SV dataset are summarized with a focus on the terms that were enriched by at least one of the 17 candidate genes related to a less aggressive behavior. For the complete results, refer to Tables S10 and S11. The total number of genes enriching each term is reported as well. The gray cells indicate that at least one of the aggressive behavior-related genes listed on the right was identified as outlier by the corresponding selection scan.

the more moderate levels in SBB. ABB population showed reduced genomic diversity and increased inbreeding levels than other European groups, compatible with the proposed demographic history of ABB characterized by population decline and isolation (Benazzo et al. 2017). ROH length distribution suggests that a large fraction of ABB genetic diversity was shaped in recent times due to inbreeding. Notably, genomic regions outside ROH still reflect the historically larger effective population size of the European brown bear metapopulation before the complete isolation of the ABB population.

The demographic analyses provided complementary perspectives on the evolutionary history of these populations. The strong bottleneck inferred for ABB a few thousand years ago supports previous work (Benazzo et al. 2017) and was likely driven by deforestation, habitat fragmentation, and land cover changes associated with the introduction and spread of agricultural technologies (Curry-Lindahl 1972; Kaplan et al. 2011; Marlon et al. 2013; Zennaro et al. 2015). This event is the most plausible explanation for the observed differences in genetic diversity between the ABB and other European brown bear populations. Although artifacts due to changes in migration rates through time or to cryptic population structure (Novo et al. 2023) could affect the reconstructed demographic history, the recent decline suggested for the SBB may be linked to the widespread bear eradication policies of the Middle Ages and/or more specifically to the Wallachian colonization. This refers to the settlement of the Carpathian Mountain areas, initiated at the end of the 12th century by the Vlachs, a pastoral ethnic group of Eastern Romance origin, who relied on sheep and goat herding for subsistence (Štofík et al. 2013).

Analyzing the genetic load attributable to SNPs in ABB and SBB, we found that ABB exhibited a lower masked load but a higher realized load compared to SBB. Assuming that most deleterious mutations have dominance coefficients close to zero (Kardos et al. 2021), the differences in homozygosity between ABB and SBB suggest that ABB individuals carry approximately twice the realized load of SBB individuals. However, future consanguineous mating would unmask more deleterious mutations in SBB than in ABB. Given that a similar pattern was observed at synonymous sites, we conservatively conclude that the contrasting patterns of genetic load at SNPs in ABB and SBB are largely shaped by their distinct demographic histories. Furthermore, we found that the age of many deleterious variants predates ABB isolation, suggesting that ABB was connected to the large west Eurasian population identified in de Jong et al. (2023), which acted as a shared reservoir of deleterious mutations that subsequently drifted in ABB contributing to its large realized genetic load.

When focusing on the genetic load from structural variation in ABB and SBB, the comparable numbers of DELs in CDS between the two populations, mostly found in the heterozygote state, suggests that only a very small number of DELs in coding regions can be tolerated in homozygosis in both populations, as they are expected to have a substantial impact on the gene product. We also observed a higher number of homozygous than heterozygous DELs in both populations at the genic and genomic levels. This pattern is unexpected in the larger SBB population and may reflect biological or technical factors. In particular, SNPs and DELs might show opposite patterns on genomic diversity. Stuart et al. (2023) found comparable or even higher SV diversity in an invasive starling population compared to two native populations but lower SNP diversity in the former (as expected because of a founder effect) and suggested that the mismatch could be due to non-mutually exclusive hypotheses like admixture, demographic expansion, and adaptation. But since our study populations have different demographic histories and live in different environments, we would not expect to observe a parallel pattern of relative genotype count at SV sites. Thus, it is possibly a technical artifact, as the easier identification of homozygous DELs than hemizygous genotypes (Plagnol et al. 2012; Parikh et al. 2016) could have led to an inflation of the former genotypic state in both populations. However, the more pronounced difference between homozygous and heterozygous DELs in ABB could reflect its demographic history of inbreeding, and this would at least partially reconcile the picture depicted by the two genetic markers.

A previous study revealed that the ABB exhibited a higher-than-expected divergence from other European bears at 22 candidate genes associated with tame/aggressive behavior (Benazzo et al. 2017). This finding suggested that the ABB could have undergone a genetically mediated shift in behavior, possibly driven by either genetic drift in its small and isolated population or by the selective hunting of more aggressive or bold individuals during long-term human–bear cohabitation in the Apennines. Here, we expanded on this analysis by conducting a blind genome-wide screening for specific signatures of local positive selection and by focusing on some interesting genes and their functions.

Three selection scan methods (RAiSD, XP-CLR, and PBS) identified in total 566 genes under putative selection. From the Tajima's *D* calculation, we found that while random genes or intergenic regions were characterized by positive values in both our target and European reference populations (ABB and SBB, respectively), consistent with theoretical expectations for declining populations, the selected genes were carrying the signature of the process of positive selection in ABB by showing a shift toward negative values. In contrast, the European population used for comparison (ie SBB) did not show this pattern, providing further support for the identification of genes uniquely varying in ABB.

The results obtained from the GO and HP enrichment analyses pointed at an actual involvement of behavior in the differentiation of ABB. Indeed, overrepresented terms like "developmental process" and "biological regulation" included selected genes with a role in the nervous system, which plays a central role in behavior. The presence of two genes involved in the glutamate pathway, namely *GRIK3* and *GRM7*, is particularly noteworthy since this neurotransmitter and its receptors have a crucial signaling role in the brain. It was suggested that the glutamate pathway was targeted during the tameness experiment conducted on the silver fox in Russia (Wang et al. 2018) and during dog (Wang et al. 2016) and cat domestication (Montague et al. 2014). Interestingly, the category "overfriendliness" conveys the idea of a docile attitude. Six out of seven genes included in this category are deleted in the Williams–Beuren syndrome, a genetic disorder in humans characterized by intellectual disability, short stature, and a heightened eagerness to interact with others (Schubert 2009). Interestingly, other two genes included in the Williams–Beuren syndrome locus were found to contribute to extreme sociability in dogs (VonHoldt et al. 2017).

Other genes putatively under selection from our analysis have been previously reported in the literature for their potential involvement in the domestication process of various animals. In the ABB genome, the genes *NUMB* and *DCC* showed signatures of positive selection, supported both by

the SNP variant dataset (Table S7) and by the presence of an intronic deletion (Table S8). *NUMB* encodes a membrane-bound endocytic adaptor protein and its potential role in the ABB behavioral shift is supported by its involvement in neurogenesis, in particular by directing cell differentiation during nervous system development (Ortega-Campos and García-Heredia 2013). Notably, an intronic variant in the human ortholog has been associated with bipolar disorder (Goes et al. 2012). According to the Mouse Genome Informatics portal (Baldarelli et al. 2024) (http://www.informatics.jax.org accessed in April 2024), *NUMB* is linked to several phenotypes involving abnormal forebrain development. Additionally, it was identified as a target of selection during horse domestication (Schubert et al. 2014). *DCC* is a netrine 1 receptor and is involved in neural crest cell migration. It was suggested to directly contribute to the development of tame behavior in various domesticated animals (Montague et al. 2014; Pendleton et al. 2018). Another strong candidate gene was *SLC13A5*. This gene has been previously linked to a genomic region associated with temperament at weaning in cattle, a measure of an animal's docility or unruliness in response to human interaction (Hulsman Hanna et al. 2014). Additionally, *SLC13A5* has been associated with several HPs related to intellectual disorders, including autism (Rigby et al. 2022).

SLC13A5, along with *DCC*, *GNAQ*, *GRM7*, *SMARCA2*, and *STX1A*, constitutes a set of candidate genes in which ABB exhibits high divergence at SNPs predicted to alter splicing factor binding motifs, including those with known roles in the brain (Table S12). Specifically, the splicing factors NOVA alternative splicing regulators 1 and 2 (*NOVA1* and *NOVA2*; Grosso et al. 2008) have been implicated in the evolution of alternative splicing patterns in the brain across vertebrates, primarily through modifications of their splicing enhancers and silencers (Jelen et al. 2007). Of particular interest, the candidate gene *DCC* stands out as a known *NOVA2* target (Saito et al. 2016).

Therefore, our results show that some variants associated with several genes, likely present as standing variation in regulatory regions before the selection occurred, might be responsible for the docile phenotype observed in the ABB. The most plausible explanation for the spread of this trait is selective culling. In other words, despite the capacity of the brown bear to implement plastic behaviors to cope with anthropogenic disturbance (Brown et al. 2023), our data support the hypothesis proposed by several authors (Festa-Bianchet and Apollonio 2003; Allendorf and Hard 2009; Martínez-Abraín et al. 2020) for harvested wild populations—that is, the more aggressive bears were eliminated, favoring the spread of genetic variants associated to reduced aggressiveness. Thus, the human population would have exerted an unintentional selective pressure on the ABB that resulted in an evolutionary adaptive change.

From a conservation perspective, a reintroduction program does not currently appear to be the most desirable management option to preserve the genetic uniqueness of the ABB and prevent ancestry loss (Benazzo et al. 2017; Maroso et al. 2023). However, if this strategy is required in the future, our results highlight the need to carefully evaluate whether to prioritize shy individuals that expand less or bold individuals that, as a drawback, may increase the likelihood of human–wildlife conflict (as discussed in Martínez-Abraín et al. 2022). For brown bears, for example, translocations involving bold/aggressive individuals can increase the chances of severe or fatal injuries to humans in case of unexpected encounters and of human-induced mortality of bear cubs and adults, as observed in the Alps (Tenan et al. 2016).

Wild populations that are able to persist in human-dominated landscapes, especially those heavily impacted by overexploitation, deserve special attention in order to study, understand, and preserve adaptations that might mitigate conflicts and promote coexistence (Oriol-Cotterill et al. 2015; Schell et al. 2021). In particular, the reduced aggressiveness of the ABB, likely due to the spread of alleles that control genetically this behavioral trait, has lowered the negative attitude toward bears in the human population that cohabits with this large mammal (Glikman et al. 2019, 2023). This, in turn, can reduce the human-caused mortality of the species. The ultimate result is the increase in the chances of population persistence in a human-dominated environment, despite an extreme drop of genomic variation and the accumulation of deleterious mutations. Therefore, even when pervasive genomic erosion has impacted a small, isolated wild population, genetic adaptations can play a crucial role in reducing the extinction risk.

Materials and Methods

Long-Read Sequencing

For the genome assembly, PacBio long reads were produced for a single ABB individual. A blood sample (500 µL) was drawn from a female Apennine bear (Lauretta) kept in captivity in the faunistic park "Centro Visita di Pescasseroli" (L'Aquila, Italy) during routine veterinary checks in 2019. The blood sample was immediately frozen in liquid nitrogen to preserve the integrity of nucleic acids. High molecular weight DNA was isolated from 200 µL of blood using the Nanobind Tissue big DNA kit (Circulomics Inc., Baltimore, USA). DNA quality and fragment length were checked in a pulse field gel electrophoresis, and DNA concentration was measured with fluorometric and spectrophotometric assays using a Qubit 2.0 Fluorometer (Invitrogen, Carlsbad, CA, USA) and a TECAN Nanoquant Infinite 200 Pro (Tecan, Mannedorf, Switzerland), respectively. Fragments of 35,000-bp length were selected using a Blue Pippin device (Sage Science, Beverly, MA, USA). Isolated fragments were used to prepare the DNA library with a SMRTbell express template prep kit 2.0 (Pacific Biosciences, Menlo Park, CA, USA) according to the manufacturer's protocols. The library was run on eight PacBio SMRT Cells 1 M in continuous long-read sequencing (CLR) mode on a PacBio Sequel platform.

Resequencing of ABB and SBB Samples

For population genomic analyses, a total of 12 and 8 *U. arctos* samples were collected in Central Italy and Slovakia, respectively. Within the 12 ABB, two cubs and their mother were included. Details of the samples are reported in Table S4. The samples were then preserved in 96% ethanol at −20 °C and the total-cell DNA was extracted using a PureLink Genomic DNA Mini Kit (Invitrogen). DNA integrity was assessed by 1.5% agarose gel electrophoresis and DNA concentration was measured using a Qubit 4 fluorometer Broad Range Assay (Invitrogen). Short-read genomic libraries were constructed using an Illumina DNA PCR-Free Prep Kit (Illumina) according to the manufacturer's protocol. Libraries were sequenced paired-end on an Illumina NovaSeq 6000 System using a 300-cycle S2 Reagent Kit v1.5, with a target coverage of 10 to 15× for all samples.

Cell Cultures, Karyotyping, and Omni-C

To confirm the chromosomal structure of our assembly, a karyotype for the ABB was generated using a cultured cell protocol. A gingival tissue biopsy was obtained from the bear Lauretta. Cells were cultured in a medium composed of 50% RPMI1640 and 50% Iscove's Modified Dulbecco's Medium, supplemented with 10% fetal bovine serum, 1% penicillin (10,000 units/mL)—streptomycin (10 mg/mL), 1% gentamycin sulfate (10 mg/mL), 0.5% amphotericin B (250 mg/mL) and 1% L-glutamine (200 mM) and incubated at 37 °C with 5% CO_2. Chromosome preparations were made following standard procedure (Stanyon and Galleni 1991). In brief, after 4 h of treatment in 0.01 ng/mL colcemid, the cells were removed by standard trypsinization and placed in a 15-mL tube. Cells were then centrifuged at 10,000 × *g*; surnatant was removed and substituted with a 1:1 mixture of 0.075 M KCl and 0.4% sodium citrate (hypotonic treatment). After a 20-min exposure at 37 °C, the cells were pelleted by centrifugation and fixed in methanol:acetic acid fixative (at a ratio of 3:1). Slides were then prepared by dropping metaphases with a Pasteur pipette onto a clean glass microscope slide. Diploid number and chromosome morphology were determined from the analyses of 20 mitotic cells stained with DAPI. Karyotype was arranged according to the standard ursid karyotype set (Nash and O'Brien 1987).

Part of the cultured cells were harvested and sent to Dovetail Genomics (Scotts Valley, CA) to construct chromatin conformation capture libraries using the Omni-C kit from Dovetail Genomics. Omni-C libraries were sequenced paired-end on an Illumina NovaSeq 6000 System using a 300-cycle Reagent Kit v1.5.

Genome Assembly

Raw PacBio CLR reads were screened with FastQC v0.11.9 (Andrews 2010) to detect the presence of residual adapter sequences and possible contaminants and trim the reads accordingly. Reads were then assembled into contigs using CSA v2.6 (Kuhl et al. 2020) with a combination of specific flags optimized for reads generated by a PacBio's Sequel instrument (-p 0 -k 15 -L5000 -S 2 -A). Before the scaffolding step within the CSA pipeline, the assembled contigs were polished with pbgcpp v2.0 (Pacific Biosciences) and POLCA v4.0 (Zimin and Salzberg 2020) using PacBio's CLR and Dovetail's Omni-C data, respectively. One round of purgedups v1.2.5 (Guan et al. 2020) was performed to remove the residual haplotype redundancy. Omni-C reads were then mapped to the scaffolds and processed according to Dovetail's documentation (https://omni-c.readthedocs.io/en/latest/index.html) using default parameters and contigs were scaffolded using SALSA v2.3 (Ghurye et al. 2017) setting the "-e DNASE" option and skipping the contigs misassembly step. The CSA pipeline was completed using the reference genome of the grizzly bear (Armstrong et al. 2022; GCA_023065955.2) to further scaffold the genome and improve contiguity. To verify that the scaffolding step using the grizzly bear genome did not introduce any misassembly due to the divergence of the two bears groups, the Omni-C reads were remapped to the final genome and PretextSuite v0.1.8 (Howe et al. 2021) was used to visually inspect the Hi-C contact maps and to manually anchor/correct scaffolds to maximize the fit of the contact data. Remaining gaps between scaffolds were closed with TGS-GapCloser 1.2.1 (Xu et al. 2020) using PacBio CLR reads. The mitochondrial sequence was reconstructed using mitoVGP pipeline v2.2 (Formenti et al. 2021) using the grizzly bear mtDNA (GCF_003584765.1) as reference and then it was manually added to the final assembly.

Transposable Element and Repeat Annotation

To identify and annotate transposable elements in the ABB genome, a de novo repeat library was constructed using the Extensive *de-novo* TE Annotator (EDTA) v1.9.9 (Ou et al. 2019). Subsequently, it was refined using DeepTE (Yan et al. 2020), which employs convolutional neural networks to classify unknown elements at the order and superfamily levels. Then the final library was used with RepeatMasker v4.1.2 (Smit et al. 2013) to mask the genome, and the RepeatMasker output files were parsed with RM_TRIPS script (https://github.com/clbutler/RM_TRIPS).

Gene Annotation

RNAseq data from closely related species available on NCBI (see Table S13) were used as evidence for the gene prediction. The quality- and adapter-trimmed RNA-seq reads were mapped to the soft-masked assembly with hisat2 v2.1.0 (Kim et al. 2015) with standard parameters followed by sorting and indexing with samtools v1.10 (Li et al. 2009). Quality control and trimming for adapters and low-quality bases (quality score <20) of the RNA-seq raw reads were performed using FastQC and TrimGalore v0.5.0 (https://github.com/FelixKrueger/TrimGalore), respectively. All the BAM files were filtered to remove invalid splice junctions with Portcullis v1.1.2 (Mapleson et al. 2018). For the prediction of gene loci and structures, the BRAKER3 pipeline v3.0.2 (Gabriel et al. 2024) was applied, which uses the soft-masked genome, filtered RNA-seq alignments and OrthoDB11 protein data (Kuznetsov et al. 2023) (https://bioinf.uni-greifswald.de/bioinf/partitioned_odb11/) as input to subsequently run the gene prediction tool GeneMark-ETP v1.00 (Bruna et al. 2024) and then AUGUSTUS v3.4.0 (Stanke et al. 2006) for its annotation process. The BRAKER transcript selector, TSEBRA v1.0.3 (Gabriel et al. 2021), was employed to unify predictions from these three sources and configured such that RNA evidence had greater weight than protein evidence. The resulting gtf file was converted to a fasta file using the perl script, gtf2aa.pl, which is included with the Augustus programming suite. To assess the completeness of the annotation, the Mammals odb10 reference database was employed in protein mode in BUSCO v5.2.2 (Manni et al. 2021). Sequences were searched in the nonredundant NCBI protein database using DIAMOND v0.9.10 (Buchfink et al. 2015) with an *E*-value cutoff of $\leq 1 \times 10^{-5}$. BLAST2GO v5.0 (Conesa et al. 2005) and INTERPROSCAN v2.5.0 (Quevillon et al. 2005) were used to assign GO terms. Protein domains were annotated by searching the InterPro v32.0 (Hunter et al. 2012) and Pfam v27.0 (Punta et al. 2012) databases, using INTERPROSCAN v5.52 and HMMER v3.3 (Finn et al. 2011), respectively.

Phylogeny

Orthologous groups in Ursidae family genomes were identified from the predicted protein sequences of the ABB and other six bear genomes already published: *U. americanus* (Supple et al. 2024), *U. maritimus* (Laidre et al. 2022), *U. thibetanus* (Zhu et al. 2020), *U. a. horribilis* (Taylor et al. 2018), *Tremarctos ornatus* (https://www.dnazoo.org/assemblies/tremarctos_ornatusC), and *Ailuropoda melanoleuca* (Fan et al. 2019). As outgroups, genomes from three Carnivora

families (Phocidae, Mustelidae, and Canidae) were added: *Neomonachus schauinslandi* (Mohr et al. 2022), *Lutra* (Mead et al. 2020), and *Canis lupus familiaris* (ROS_Cfam_1.0; GCF_014441545.1). When several alternatively spliced transcripts of a gene were annotated, the longest transcript was considered to represent the gene model. A series of tools was used to cluster proteins into orthogroups, reconstruct gene trees, and estimate the species tree: ORTHOFINDER v2.5.4 (Emms and Kelly 2019), DIAMOND v0.9.14, Multiple Alignment using Fast Fourier Transform (MAFFT) v7.305 (Katoh and Standley 2013), and RAxML v8.2.12 (Stamatakis 2014).

Synteny

The syntenic relationship within Carnivora was evaluated comparing the ABB genome with the grizzly bear and eight other species having a chromosome-scale reference genome from NCBI or DNAzoo (Dudchenko et al. 2017, 2018) repositories including *U. americanus*, *U. maritimus*, *U. a. horribilis*, *Tremarctos ornatus*, *Ailuropoda melanoleuca*, *Neomonachus schauinslandi*, *Arctocephalus gazella*, *Lutra*, and *C. l. familiaris*. BUSCO v5.0.0 was used to scan each genome using the carnivora_odb10 database and all complete single-copy genes shared among species were extracted for comparative analysis. The coordinates of each BUSCO gene were traced between species using the software RIdeogram v0.2.2 (Hao et al. 2020). Large structural variants characterizing the genome of the five bear species were identified and visualized using syri v1.7 (Goel et al. 2019) and plotsr v1.1 (Goel and Schneeberger 2022), respectively.

MHC Inversion

The presence of a rearrangement on Scaffold_31 was assessed using region-specific amplification followed by Sanger sequencing. Specifically, a primer pair was designed to amplify the region across the putative breakpoint of the scaffold followed by the inverted region based on the latest assembly of the ABB genome. The forward primer annealed 1,066-bp upstream of the breakpoint (Umar_inv_F1 5′-GTCATTCATGGCCAGG GAAC-3′), while the reverse primer annealed 1,922-bp downstream of the breakpoint (Umar_inv_R1 5′-GCTCTGAC TCCTTCCACCAT-3′), allowing the amplification of a 2,989-bp fragment. The primer pair was used in a PCR reaction with 1.25 units of the enzyme PrimeSTAR GXL DNA Polymerase (Takara), 30 cycles with annealing at 58 °C for 15 s and extension at 68 °C for 3 min. The resulting PCR products were then purified and Sanger sequenced with a combination of internal primers (Umar_inv_R2 5′-CATAACCACA CAGCCAGCAA-3′; Umar_inv_R3 5′-CATGCTGTCAT CCCCAAAGG-3′; Umar_inv_F3 5′-GCTTAACCAACTGAG CCACC-3′) to confirm the inversion. The analysis was carried out on four ABB including Lauretta, two samples from Slovakia, and one sample from the Italian Alps. To further validate the inversion, the read mapping distribution along the region of Scaffold_31 was generated aligning short and long reads to the reference genome using bwa v0.7.17 and minimap2 v2.22, respectively. The genomic tracks showing the sequencing coverage were generated from the alignments using plotsr v1.1.

SNP Variant Calling

For population-level brown bears samples, the newly produced reference genome of the ABB was used for mapping: 20 individuals resequenced for the purpose of this study (including 12 ABB and 8 SBB), and 9 brown bear individuals from Europe already available (including 1 ABB and 1 SBB) (Liu et al. 2014; Benazzo et al. 2017; Barlow et al. 2018). Moreover, three polar bear individuals (Liu et al. 2014) were mapped to the polar bear genome (GCF_017311325.1: 3,900 scaffolds, total length = 2,330,485,043 bp) and three black bear individuals (Miller et al. 2012; Cahill et al. 2013; Srivastava et al. 2019) to the black bear genome (GCF_020975775.1: 105 scaffolds longer than 50,000 bp and covering 2,328,269,719 bp, ie 90% of the genome length was used). All reads were mapped to the corresponding reference genome using BWA-mem v0.7.17 (Li et al. 2009) with default parameters, with an optical density value of 2,500 for the samples generated in our study that used patterned flow cells and 100 for the other individuals. Reads were merged prior to mapping using AdapterRemoval v2.3.1 (Schubert et al. 2016) when the sequencing strategy generated overlapping reads. PCR and optical duplicates were tagged using MarkDuplicate from Picard v2.24.1 (http://broadinstitute.github.io/picard). For the individuals sequenced in this study, a PCR-free sequencing kit was used, so reads tagged as PCR duplicates were further untagged using a custom bash script. Diverse statistics were computed to ensure the quality of the mapping.

An independent SNP calling was performed for each of the three species. SNP calling was performed using GATK v4.1.9.0 (McKenna et al. 2010) following the best practice guides for short variant discovery, composed of three steps: calling variants per sample using HaplotypeCaller; consolidating GVCFs to improve scalability using GenomicsDBImport; joint-genotyping all the per-sample GVCFs using GenotypeGVCFs. HaplotypeCaller was run independently in each scaffold of each individual, using the option EMIT_ALL_CONFIDENT_SITES to output all sites (including nonvariant sites), and the output was generated in condensed nonvariant blocks. A minimum mapping quality of 20 was used. GenomicsDBImport and GenotypeGVCFs were run independently for each scaffold. The tag --include-non-variant-sites was used in GenotypeGVCFs to output all sites (including nonvariant sites). For the brown bears, all scaffolds were cut into windows of 10 Mb using bedtools v2.30 makewindow (Quinlan and Hall 2010), and each window was run independently to satisfy memory requirements. Finally, all the windows and scaffolds were merged to produce one unique VCF file per dataset using bcftools merge v1.11 (Li 2011).

From the raw VCF file produced after SNP calling, first extracted SNPs and indels were extracted using GATK SelectVariant. Indels were filtered by quality (minimum quality of 60) and then used to filter out SNPs located within 5 bp of the high-quality indels, and that fulfilled the following criteria: QUAL < 60; QD < 2.0; FS > 60.0; MQ < 40.0; MQRankSum < −20.0; ReadPosRankSum < −8.0; DP < mean depth/3; DP > mean depth × 2; GQ < 10. The mean depth was computed from samtools v1.11 depth at each position. Invariant sites were extracted using GATK SelectVariant and further filtered using GATK VariantFiltration to remove genotypes with RGQ < 10. Finally, high-quality variant and invariant sites were merged using bcftools concat.

The three reference genomes used for read mapping were aligned to identify syntenic regions that could be safely associated and used in every analysis involving a comparison between species. The aim of this procedure was to remove the

reference bias associated with short-read mapping toward a single reference and to exclude variants located within, or in proximity of, genomic regions involved in cross-species rearrangements. The polar and the black bear genomes were aligned to the ABB reference using minimap2 v2.22 (Li 2018), setting a maximum divergence of 5% and adding the "cs" tag. Transanno v0.2.4 (https://github.com/linformationsea/transanno) was then used to produce a chain file from minimap2 output, to extract well-aligned regions between reference genomes, and to lift the genomic coordinates of all sites (monomorphic and polymorphic) contained in the VCF files between species. The lifted VCF files for each species, all of them following the ABB genome coordinate system, were merged using bcftools, retaining only sites for which the liftover procedure between species was possible and excluding sites completely missing in all individuals belonging to one or more species.

Structural Variants Calling

SV calling was performed on the genomes of 11 ABB from Central Italy (mother–daughter pair excluded), 9 SBB, 8 grizzly bears from Canada (de Jong et al. 2023), and 6 grizzly bears from Alaska (Miller et al. 2012; Cahill et al. 2013; de Jong et al. 2023). To avoid reference bias, all reads were mapped to the polar bear (*U. maritimus*) reference genome using the same procedure detailed for SNP calling. The SV calling was performed with the meta-method Parliament2 v0.1.11 (Zarate et al. 2021) that incorporates multiple preinstalled SV callers to identify high-quality SVs starting from short-reads genomic data. Different preinstalled SV callers were selected in order to detect different types of SVs (deletions, duplications, insertions, and inversions) using different signals (paired-end reads, split reads, and read depth): BreakDancer (Chen et al. 2009), CNVnator (Abyzov et al. 2011), Lumpy (Layer et al. 2014), Delly (Rausch et al. 2012), and Manta (Chen et al. 2016). To identify the SVs in each individual's genome, Parliament2 requires the BAM file and the reference genome used for the alignment. The SV calling was limited to scaffolds longer than 1 Mb with the option --filter_short_contigs. Next we used SURVIVOR v1.0.6 (StructURal Variant majorIty VOte) (Jeffares et al. 2017), in its option "merge," to obtain a consensus of the SVs identified by each method. Parameters have been set to maintain only SVs longer than 50 bp called by at least 2 SV callers out of 5 and to group as single SV those with the same type and a maximum difference of 1,000 bp between starting and ending positions without considering the genotype. Then, SURVIVOR merge was used to obtain a multi-sample VCF with all the SVs identified in at least 1 individual out of 35. Then SVs with low-quality value (GQ < 20) and that were no longer identified in at least one individual (flag –max-missing-count) were filtered out with vcftools v0.1.16 (Danecek et al. 2011). No SVs shared between all individuals and with a distance between the starting and ending positions longer than 10 Mb were allowed. Only for duplications and inversions, bedtools merge and intersect were used to filter out in case of partial overlap in all individuals.

Species Phylogeny and Genomic Diversity

The maternal lineage was reconstructed through mtDNA, mapping raw reads with the read alignment procedures previously described for the resequencing data. For each male, the consensus sequences were generated with bcftools mpileup v1.10.2-9, filtering out bases with low phred-scaled quality scores ($Q < 20$) and reads with low mapping quality ($q < 40$). An alignment totaling 13,882 bp, which included only coding regions and rRNA (12S and 16S), was used in the analysis. The phylogeny was reconstructed using a neighbor-joining tree implemented in Geneious 8.1 (Kearse et al. 2012) with GTR + alpha substitution model. The black bear was used to root the tree.

The DNA nuclear phylogeny was reconstructed starting from pairwise genetic distances between individuals using the function --distance square 1-ibs implemented in PLINK v1.90 (Purcell et al. 2007) for 34 individuals at 24,868,223 positions. A neighbor-joining phylogenetic tree was then estimated from the pairwise distance matrix using the package ape (Paradis and Schliep 2019) in R v4.0.

Genomic diversity was investigated through different statistics (number of SNPs, heterozygosity) in the studied populations. ROHs were inferred with ROHan v1.0 (Renaud et al. 2019). To obtain an estimate of the maximum heterozygosity level permitted in ROH regions, ROHan was run on the chromosome X for all male individuals, removing the first 11 Mb that exhibited an abnormal high heterozygosity level and excluding repeated regions. After obtaining a mean heterozygosity of 1.36×10^{-4}, a rohmu value (the inferred heterozygosity rate) of 1×10^{-4} was used to define regions in ROH in the autosomes for all ABB and SBB populations. The analysis was conducted using a window size of 100 kb. As a commonly used proxy for the inbreeding coefficient, the fraction of the total genome assigned to ROHs (F_{ROH}) was then computed. Additionally, the distribution of different ROH lengths was estimated from ROHan output files. The estimation of the number of generations since inbreeding events was obtained from the formula $g = 100/(2rL)$, where r is the recombination rate (1 cM/Mb) and L is the ROH length in Mb (Thompson 2013). Based on this, the following estimates were obtained: an ROH length of 100 kb corresponds to ~500 generations, 1 Mb to ~50 generations, 2 Mb to ~25 generations, and 5 Mb to ~10 generations. ROHan was also used to estimate Watterson's θ both including and excluding ROH regions.

Demography

The long-term variation in population size was investigated using PSMC v0.6.5 (Li and Durbin 2011) following the standard procedure for the three individuals with highest depth of coverage for ABB and SBB, respectively. SNPs were called from the BAM files for each of the 37 scaffolds longer than 10 Mb using bcftools mpileup and bcftools call, only using positions with a minimum base and mapping quality of 30 and covered between one-third and two times the mean individual depth. Windows of 100 bp were then used to produce the PSMC input. The default time patterning ("4 + 25 × 2 + 4 + 6") was used, with an initial theta/rho ratio (-*r* parameter) of 5 and a maximum $2N_0$ coalescent time (-*N* parameter) of 15 (default values). One hundred rounds of bootstrapping were performed by randomly sampling with replacement from 5 Mb sequences. A generation time of 11 years and a mutation rate of 1.82×10^{-8} per site per year (Liu et al. 2014; Benazzo et al. 2017) were used for plotting.

Since the PSMC does not infer recent N_e variation (<400 generations), a different method was used to infer recent changes in N_e that might have influenced the ABB population in comparison to its SBB counterpart. In particular, GONE v1.0 (Santiago et al. 2020), a method based on linkage

disequilibrium, was used. GONE was run for the 11 ABB (excluding the mother–daughter pair) and 9 SBB to estimate recent demographic history in European brown bears. Default parameters were used except for $hc = 0.01$ (Nadachowska-Brzyska et al. 2021; Bazzicalupo et al. 2022). We performed ten independent replicates for each population to evaluate the consistency of the estimations.

Mutation Load

Each SNP was polarized as ancestral or derived using two outgroups: the polar bear (three individuals) and the black bear (three individuals). The ancestral allele was defined as the allele present in at least two out of three polar bear individuals and in at least two out of three black bear individuals using a custom python script. All sites where at least one of these outgroups was heterozygous were discarded to maximize the confidence in the ancestral allele definition.

The mutational load was assessed in both 11 ABB (mother–daughter pair excluded) and 9 SBB through two distinct methods. Only protein coding sequences (CDS) were analyzed, extracting the CDS of the longest transcript of each gene of the annotation and merging the overlapping windows with bedtools, resulting in a total CDS length of 33 Mb. First, the relative mutational load was measured in each individual as the number of derived alleles at sites that are under strict evolutionary constraints (ie highly conserved) and thus likely to be deleterious using Genomic Evolutionary Rate Profiling (GERP) scores (Cooper et al. 2005). GERP scores for the polar bear in bigwig format was obtained from a multiple alignment with 91 mammal species downloaded from ENSEMBL (https://ftp.ensembl.org/pub/release-114/compara/conservation_scores/91_mammals.gerp_conservation_score/). First the ABB assembly was aligned to the polar bear assembly using minimap2 with parameter -cx asm20. The GERP scores were subsequently transferred to ABB reference coordinates using Transanno between the polar bear and the ABB genome. Our analysis considered both heterozygous positions (counted as one allele) and homozygous positions (counted as two alleles), recognizing that the mutational impact of heterozygous positions involves additional assumptions regarding the dominance coefficient. GERP identifies constrained elements within multiple alignments by quantifying substitution deficits, reflecting substitutions that would have occurred if the element was neutral DNA but did not due to functional constraints, accounting for phylogenetic divergence. The individual relative mutational load was calculated by summing the number of derived alleles above a GERP score of 4 (highly deleterious).

Secondly, SnpEff v5.0 (Cingolani et al. 2012) was run on the polarized SNPs present in CDS to classify each mutation as synonymous, missense (ie nonsynonymous) or nonsense (including stop-gained, start-gained, start lost, stop codons, splice donor variant, and splice acceptors). For each class of putatively deleterious mutation (missense and nonsense mutations), the genetic load was separated into two components: (i) the masked load estimated as the individual number of heterozygous sites, and (ii) the realized load estimated as the individual number of homozygous derived sites (Bertorelle et al. 2022).

The age of deleterious and neutral alleles was estimated by inferring the time to the most recent common ancestor of those mutations with Genealogical Estimation of Variant Age (GEVA) (Albers and McVean 2020), which reconstructs a genealogical tree at the chromosomal level of variable sites and estimates the age of genetic variants by identifying segments that are shared between a pair of haplotypes. It assumes that an allele originates from a mutation event on the genome of a common ancestor, and it is subsequently passed down to all descendant haplotypes. The time of origin of a mutation is obtained by a probabilistic estimate that combines the cumulative distributions for pairs of haplotypes that share the mutation ("concordant pairs") and the pairs that do not ("discordant pairs") (Albers and McVean 2020). Since GEVA requires phased data, SNPs were phased with BEAGLE v5.4 (Browning et al. 2021), using the options impute = false, $N_e = 10{,}000$, burn-in = 15, iteration = 40, and phase-states = 300. Singletons, private doubletons, and sites with more than 10% of missingness were excluded from the analysis with vcftools. We used an effective population size of 10,000, a recombination rate of 1.0×10^{-8}, and a mutation rate of 1.82×10^{-8} per site per year.

The genetic load attributable to the SVs was also investigated by comparing the amount and distribution of DELs in the ABB and the SBB populations. We first kept only the samples from those two populations (11 ABB and 9 SBB) from the merged dataset, and selected only DELs as a proxy of the SV dataset being the most abundant SV category (82% on average per individual). To exclude the SVs accumulated from the separation between the brown bears and the polar bear (used as reference genome), SVs with a frequency greater than or equal to 0.85 were filtered out, considering them fixed but not identified in all 20 samples due to methodological limitations in SV identification with low-medium coverage. Starting from the individual genotyped VCFs produced by Lumpy and genotyped by SVTyper (Chiang et al. 2015) during the SV calling step, only the DELs that were included in the 20 samples merged SV dataset were selected, as these were considered high-quality SVs. For each individual, the number of DELs, and the derived homozygous and heterozygous genotypes were quantified considering the whole genome, the genes, and the CDS. To further analyze the characteristics of genes affected by homozygous and heterozygous DELs, the number of protein–protein interactions was considered as a proxy for gene importance (Chen et al. 2020; Liang et al. 2024). The protein–protein interaction database for the polar bear was downloaded from STRING (Szklarczyk et al. 2023), which lists all interactions between proteins, in order to calculate the number of interactions for each gene product with a minimum confidence score of 0.4. The number of interactions of the gene products of genes impacted by both homozygous and heterozygous DELs in their CDS or in their intronic regions and the mean number of interactions for all the gene products listed by STRING was quantified. Then, the mean numbers of interactions were compared with a Mann–Whitney U test.

Selection Scans

A series of analyses was implemented to detect selection in the ABB. As this small population has likely experienced considerable levels of genetic drift that can leave confounding signatures to the ones of positive selection, the number of populations studied and the number of approaches were increased in the attempt to infer positive selection. The ABB samples analyzed included 11 individuals: the mother–daughter pair was excluded from the 12 new sequences and one medium-coverage individual was included from a previous

study (Benazzo et al. 2017). The SBB sample included the eight newly sequenced individuals and one medium-coverage individual from a previous study (Benazzo et al. 2017). Fifteen individuals from grizzly brown bears (nine from Canada, six from Alaska) were included to compare North American to European populations. For these new samples, the same procedure as described above was followed for read mapping (to the ABB reference genome), SNP calling, and filtering, including all brown bear individuals. This new dataset comprised 35 individuals (see Table S4) and 12,906,067 SNPs.

To detect signatures of recent positive selection at the population level, the first method applied was RAiSD v2.9 (Alachiotis and Pavlidis 2018). RAiSD detects positive selection based on multiple signatures of selective sweeps, namely the change in the Site Frequency Spectrum, the levels of linkage disequilibrium, and the amount of genetic diversity along a chromosome, scoring these three components into the *μ statistic*. The analysis was applied to all brown bear populations to select candidate genes under positive selection exclusive to the ABB. RAiSD was run with the default parameters on overlapping sliding windows of 20 SNP with a 1-SNP sliding interval, which were then converted into nonoverlapping windows of 50 kb using bedtools in order to obtain the same genomic windows as in the other analyses to facilitate comparisons between different results.

A second method to identify regions of the genome under selection was the XP-CLR, which detects selective sweeps in pairs of populations by searching for extreme allele frequency differentiation over genomic windows. Values were calculated per chromosome using xpclr v1.1.2 (Chen et al. 2010) on the dataset with all samples after quality filtering. We used nonoverlapping windows of 50 kb (–size 50,000 --step 50,000) in the pairwise comparisons.

Finally, the PBS was implemented using four populations, as illustrated in Jiang et al. (Jiang and Assis 2020), to look for genomic regions specifically differentiated in the ABB compared to the European and North American samples. Mean pairwise F_{ST} values were computed in nonoverlapping 50 kb windows with vcftools, setting to zero the negative indexes and to 0.99 the fixed differences to avoid infinite branch length. Then the Cavalli-Sforza transformation was applied to obtain the PBS values with the following equation:

$$\mathrm{PBS} = \frac{2 \times d\,(\mathrm{MAR} - \mathrm{SLO}) \; + \; d\,(\mathrm{MAR} - \mathrm{CAN}) \; + \; d(\mathrm{MAR} - \mathrm{ALA}) - \; d(\mathrm{SLO} - \mathrm{CAN}) - d(\mathrm{SLO} - \mathrm{ALA})}{4}$$

where d is the log-transformed distance between two populations. The windows showing a negative PBS, which can be obtained in case of small sample size, were set to zero as they do not have a biological meaning. This last method was applied to the SV datasets as well. The only procedural difference concerned the F_{ST} calculation that for the SVs was done on each marker rather than in a sliding window fashion.

To identify a potential list of regions under selection and contribute to understanding how selection has affected the genomic variation in ABB, outliers were defined following a similar procedure for each analysis (RAiSD, XP-CLR, and PBS), and all outlier genes were combined to get a list of candidate genes under selection in the ABB. The top 1% windows were computed for each analysis. Then, for the SNP dataset, outlier windows were merged when less distant than 100 kb from each other. Finally, genes present in these outlier windows or regions were extracted by blasting the ABB transcripts to the dog genes. As some analyses were run to get candidate regions under positive selection in the ABB population and others were run as a control in the remaining populations, the final list of candidate genes was obtained by considering only the outliers in ABB from RAiSD and PBS or in the ABB–SBB comparison from XP-CLR that were not outliers in the other control analyses (ie RAiSD for the SBB, Canadian brown bear, or Alaskan brown bear, or XP-CLR for the ABB/Canadian brown bear or ABB/Alaskan brown bear). Then, GO and HP enrichment analysis were performed with g:Profiler (Kolberg et al. 2023) for candidate genes identified for all three analyses combined together using the dog gene set. As the GO enrichment analysis might not identify pathways related to selection affecting a few genes of major effect, an extensive review of the function of the candidate genes present in at least one of the three selection scan analyses was performed as well.

Similarly, for the PBS analysis on the SV dataset, the SVs in the top 1% carrying the derived allele in the ABB population were considered outliers, and a separate GO enrichment analysis on g:Profiler was conducted using the available polar bear gene set.

All the selection scans and GO enrichment analysis above were repeated using the SBB as the target population in order to verify if the signatures of selection identified in the ABB were the result of a true signal specific to that population. Moreover, Tajima's D was computed in 50-kb windows with vcftools to verify whether the whole ensemble of candidate genes under selection in the ABB were behaving differently from the same number of random genes or intergenic regions while a different pattern could be expected in the SBB.

One of the phenotypes that distinguishes the ABB from the other brown bear populations, ie reduced aggressiveness toward humans, was selected for further investigation. Therefore, a list of 17 candidate genes under selection (see Results) was found to have a putative role in the determination of this phenotype, and was analyzed in more detail to possibly unveil the molecular mechanism responsible for the less aggressive attitude of the ABB. After noticing that most of the genetic variation was found in intronic regions rather than in coding portions of the candidate genes (Table 1), a series of in silico analyses was applied to investigate the potential alteration of splicing at the abovementioned genes. Genes were scanned for SNPs that could alter the acceptor/donor sites recognition during pre-mRNA maturation with SpliceAI (Jaganathan et al. 2019). This program was shown to perform better than many other tools (Riepe et al. 2021) especially for deep intronic variants because of the large windows provided during the training of its deep learning model (Jaganathan et al. 2019) and has already been applied to species other than *Homo sapiens* (Brand et al. 2023). The analysis was applied on the maximum window length allowed (ie 10 kb) and SNPs with delta score > 0.2 were considered potential splice-altering sites.

Another feature that can lead to alternative splicing is the alteration of splicing factor site recognition. Two different tools were used to explore this process: HOT-SKIP (Raponi et al. 2011) was developed to score exonic variants for their probability of inducing exon skipping; SpliceAid2 (Piva et al. 2012) allows to identify RNA-binding protein target motifs. As these programs are available as web interface only, the number of SNPs to analyze was limited by considering only

Table 1 Selected genes putatively under selection and with possible role in the modification of behavior in the Apennine brown bear (ABB)

Gene	Criterion	# highly differentiated SNPs int/syn/nsyn	Donor/acceptor splicing site gain/loss	Modifications to splicing factor binding motifs
ASTN1	Other neural functions	37/0/0	0	n.a.
BPTF	Tame list	3/0/0	0	3
BUD23	Enrichment	1/0/0	0	1
DCC	Tame list	61/0/0	0	223
DNAJC30	Enrichment	0/0/0	0	n.a.
GABRB2	Other neural functions	3/0/0	0	n.a.
GNAQ	Tame list	86/0/0	0	65
GRIK3	Tame list	122/1/0	0	n.a.
GRM7	Tame list	409/0/0	0	311
METTL27	Enrichment	1/0/0	0	1
NUMB	Other neural functions	4/0/0	0	n.a.
OXTR	Tame list	34/0/0	0	26
SLC13A5	Other neural functions	9/1/0	1	10
SMARCA2	Enrichment	72/1/0	1	62
STX1A	Enrichment	3/0/0	0	2
TMEM270	Enrichment	0/0/0	0	n.a.
VPS37D	Enrichment	0/0/0	0	n.a.

The genes are reported together with the criterion for their inclusion in this list. The number of highly differentiated SNPs in intronic (int) and exonic (synonymous: syn; nonsynonymous: nsyn) regions is reported. Splicing alterations predicted for the highly differentiated SNPs were divided into two different mechanisms involved in pre-mRNA maturation: the gain or loss of donor or acceptor sites for intron excision and the modification of splicing factor binding motifs. Note that sequence motifs recognized by different splicing factors can be similar and overlapping, hence one SNP can cause the modification or disruption of more than one splicing factor binding site. This analysis was conducted only on the most promising genes in terms of their function and differentiation between ABB and the other brown bears.

the most promising genes and retaining the SNPs with $F_{ST} \geq$ 0.73, 0.89, and 0.80 between ABB and SBB, Canadian and Alaskan bears, respectively (top 10% in each comparison).

Supplementary material

Supplementary material is available at *Molecular Biology and Evolution* online.

Acknowledgments

We thank the Huck Institutes of Life Sciences and Penn State Altoona for the funding provided for G.F. We also thank Leonardo Gentile and the National Park of Abruzzo Lazio and Molise for their assistance during sampling activities and Elisa Desiato for her help in the splicing analysis.

Author Contributions

A.B. and G.B. conceived the study. L.P., A.B., and G.B. coordinated and performed sample collection. A.I. performed laboratory work. M.S. and M.Ge. performed Hi-C data generation and analysis. G.F., R.B., M.Ga., B.S., S.T.V., P.S., L.A., G.P., M.S., and A.I. performed the analyses. G.F., R.B., M.Ga., B.S., S.F., S.T.V., P.S., A.I., A.B., and G.B. wrote the paper. All authors read, revised, and approved the manuscript.

Funding

This work was supported by the University of Ferrara (Italy) and funded by the MIUR PRIN 2017 grant 201794ZXTL to G.B.; S.T.V. was supported by a Young Researchers (Marie Skłodowska-Curie winners) grant awarded by the Italian Ministry for Universities and Research. P.C. was supported by the European Union—NextGenerationEU National Biodiversity Future Center.

Data Availability

The genome raw reads and the genome assembly are available at the National Center for Biotechnology Information (NCBI) with the BioProject no. PRJNA1247790. The genome assembly and annotation are available for download from Zenodo (https://doi.org/10.5281/zenodo.15349716). Analysis scripts are publicly available on GitHub (https://github.com/POPGG-UniFe/Uarctos_popgen).

References

Abyzov A, Urban AE, Snyder M, Gerstein M. CNVnator: an approach to discover, genotype, and characterize typical and atypical CNVs from family and population genome sequencing. *Genome Res*. 2011:21:974–984. https://doi.org/10.1101/gr.114876.110.

Alachiotis N, Pavlidis P. RAiSD detects positive selection based on multiple signatures of a selective sweep and SNP vectors. *Commun Biol*. 2018:1:79. https://doi.org/10.1038/s42003-018-0085-8.

Albers PK, McVean G. Dating genomic variants and shared ancestry in population-scale sequencing data. *PLoS Biol*. 2020:18:e3000586. https://doi.org/10.1371/journal.pbio.3000586.

Albrecht J *et al*. Humans and climate change drove the Holocene decline of the brown bear. *Sci Rep*. 2017:7:1–11. https://doi.org/10.1038/s41598-017-10772-6.

Allendorf FW, Hard JJ. Human-induced evolution caused by unnatural selection through harvest of wild animals. *Proc Natl Acad Sci U S A*. 2009:106:9987–9994. https://doi.org/10.1073/pnas.0901069106.

Andrews S. FastQC: A Quality Control tool for High Throughput Sequence Data. 2010.

Armstrong EE *et al*. A beary good genome: haplotype-resolved, chromosome-level assembly of the brown bear (*Ursus arctos*). *Genome Biol Evol*. 2022:14:evac125. https://doi.org/10.1093/gbe/evac125.

Baldarelli RM *et al*. Mouse genome informatics: an integrated knowledgebase system for the laboratory mouse. *Genetics*. 2024:227:iyae031. https://doi.org/10.1093/genetics/iyae031.

Barlow A *et al*. Partial genomic survival of cave bears in living brown bears. *Nat Ecol Evol*. 2018:2:1563–1570. https://doi.org/10.1038/s41559-018-0654-8.

Bazzicalupo E *et al*. History, demography and genetic status of Balkan and Caucasian *Lynx* (Linnaeus, 1758) populations revealed by genome-wide variation. *Divers Distrib*. 2022:28:65–82. https://doi.org/10.1111/ddi.13439.

Beckman AK, Richey BMS, Rosenthal GG. Behavioral responses of wild animals to anthropogenic change: insights from domestication. *Behav Ecol Sociobiol*. 2022:76:105. https://doi.org/10.1007/s00265-022-03205-6.

Benazzo A *et al.* Survival and divergence in a small group: the extraordinary genomic history of the endangered Apennine brown bear stragglers. *Proc Natl Acad Sci U S A*. 2017:114:E9589–E9597. https://doi.org/10.1073/pnas.1707279114.

Bertorelle G *et al.* Genetic load: genomic estimates and applications in non-model animals. *Nat Rev Genet*. 2022:23:492–503. https://doi.org/10.1038/s41576-022-00448-x.

Bombieri G *et al.* Towards understanding bold behaviour of large carnivores: the case of brown bears in human-modified landscapes. *Anim Conserv*. 2021:24:783–797. https://doi.org/10.1111/acv.12680.

Brand CM, Colbran LL, Capra JA. Resurrecting the alternative splicing landscape of archaic hominins using machine learning. *Nat Ecol Evol*. 2023:7:939–953. https://doi.org/10.1038/s41559-023-02053-5.

Breck SW, Poessel SA, Mahoney P, Young JK. The intrepid urban coyote: a comparison of bold and exploratory behavior in coyotes from urban and rural environments. *Sci Rep*. 2019:9:1–11. https://doi.org/10.1038/s41598-019-38543-5.

Brown L *et al.* Landscape of fear or landscape of food? Moose hunting triggers an antipredator response in brown bears. *Ecol Appl*. 2023:33:e2840. https://doi.org/10.1002/eap.2840.

Browning BL, Tian X, Zhou Y, Browning SR. Fast two-stage phasing of large-scale sequence data. *Am J Hum Genet*. 2021:108:1880–1890. https://doi.org/10.1016/j.ajhg.2021.08.005.

Brůna T, Lomsadze A, Borodovsky M. GeneMark-ETP significantly improves the accuracy of automatic annotation of large eukaryotic genomes. *Genome Res*. 2024:34:757–768. https://doi.org/10.1101/gr.278373.123.

Buchfink B, Xie C, Huson DH. Fast and sensitive protein alignment using DIAMOND. *Nat Methods*. 2015:12:59–60. https://doi.org/10.1038/nmeth.3176.

Cahill JA *et al.* Genomic evidence for island population conversion resolves conflicting theories of polar bear evolution. *PLoS Genet*. 2013:9:e1003345. https://doi.org/10.1371/journal.pgen.1003345.

Charmantier A, Gienapp P. Climate change and timing of avian breeding and migration: evolutionary versus plastic changes. *Evol Appl*. 2014:7:15–28. https://doi.org/10.1111/eva.12126.

Chen H *et al.* New insights on human essential genes based on integrated analysis and the construction of the HEGIAP web-based platform. *Brief Bioinform*. 2020:21:1397–1410. https://doi.org/10.1093/bib/bbz072.

Chen H, Patterson N, Reich D. Population differentiation as a test for selective sweeps. *Genome Res*. 2010:20:393–402. https://doi.org/10.1101/gr.100545.109.

Chen K *et al.* BreakDancer: an algorithm for high-resolution mapping of genomic structural variation. *Nat Methods*. 2009:6:677–681. https://doi.org/10.1038/nmeth.1363.

Chen X *et al.* Manta: rapid detection of structural variants and indels for germline and cancer sequencing applications. *Bioinformatics*. 2016:32:1220–1222. https://doi.org/10.1093/bioinformatics/btv710.

Chiang C *et al.* SpeedSeq: ultra-fast personal genome analysis and interpretation. *Nat Methods*. 2015:12:966–968. https://doi.org/10.1038/nmeth.3505.

Cingolani P *et al.* A program for annotating and predicting the effects of single nucleotide polymorphisms, SnpEff: SNPs in the genome of *Drosophila melanogaster* strain w1118; iso-2; iso-3. *Fly (Austin)*. 2012:6:80–92. https://doi.org/10.4161/fly.19695.

Ciucci P *et al.* Estimating abundance of the remnant Apennine brown bear population using multiple noninvasive genetic data sources. *J Mammal*. 2015:96:206–220. https://doi.org/10.1093/jmammal/gyu029.

Colangelo P *et al.* Cranial distinctiveness in the Apennine brown bear: genetic drift effect or ecophenotypic adaptation? *Biol J Linn Soc*. 2012:107:15–26. https://doi.org/10.1111/j.1095-8312.2012.01926.x.

Conesa A *et al.* Blast2GO: a universal tool for annotation, visualization and analysis in functional genomics research. *Bioinformatics*. 2005:21:3674–3676. https://doi.org/10.1093/bioinformatics/bti610.

Cooper GM *et al.* Distribution and intensity of constraint in mammalian genomic sequence. *Genome Res*. 2005:15:901–913. https://doi.org/10.1101/gr.3577405.

Corbo M, Damas J, Bursell MG, Lewin HA. Conservation of chromatin conformation in carnivores. *Proc Natl Acad Sci U S A*. 2022:119:e2120555119. https://doi.org/10.1073/pnas.2120555119.

Curry-Lindahl K. The brown bear (*Ursus arctos*) in Europe: decline, present distribution, biology and ecology. *Bears Their Biol Manag*. 1972:2:74. https://doi.org/10.2307/3872571.

Danecek P *et al.* The variant call format and VCFtools. *Bioinformatics*. 2011:27:2156–2158. https://doi.org/10.1093/bioinformatics/btr330.

Davison J *et al.* Late-quaternary biogeographic scenarios for the brown bear (*Ursus arctos*), a wild mammal model species. *Quat Sci Rev*. 2011:30:418–430. https://doi.org/10.1016/j.quascirev.2010.11.023.

de Jong MJ *et al.* Range-wide whole-genome resequencing of the brown bear reveals drivers of intraspecies divergence. *Commun Biol*. 2023:6:153. https://doi.org/10.1038/s42003-023-04514-w.

Donihue CM, Lambert MR. Adaptive evolution in urban ecosystems. *Ambio*. 2015:44:194–203. https://doi.org/10.1007/s13280-014-0547-2.

Dudchenko O *et al.* The Juicebox Assembly Tools module facilitates *de novo* assembly of mammalian genomes with chromosome-length scaffolds for under $1000. bioRxiv 254797. https://doi.org/10.1101/254797, 28 January 2018, preprint: not peer reviewed.

Dudchenko O *et al.* De novo assembly of the *Aedes aegypti* genome using Hi-C yields chromosome-length scaffolds. *Science*. 2017:356:92–95. https://doi.org/10.1126/science.aal3327.

Eizaguirre C, Lenz TL, Traulsen A, Milinski M. Speciation accelerated and stabilized by pleiotropic major histocompatibility complex immunogenes. *Ecol Lett*. 2009:12:5–12. https://doi.org/10.1111/j.1461-0248.2008.01247.x.

Emms DM, Kelly S. OrthoFinder: phylogenetic orthology inference for comparative genomics. *Genome Biol*. 2019:20:1–14. https://doi.org/10.1186/s13059-019-1832-y.

Epplett C. The capture of animals by the roman military. *Greece Rome*. 2001:48:210–222. https://doi.org/10.1093/gr/48.2.210.

Fallahsharoudi A *et al.* QTL mapping of stress related gene expression in a cross between domesticated chickens and ancestral red junglefowl. *Mol Cell Endocrinol*. 2017:446:52–58. https://doi.org/10.1016/j.mce.2017.02.010.

Fam BSO *et al.* Oxytocin and arginine vasopressin systems in the domestication process. *Genet Mol Biol*. 2018:41:235–242. https://doi.org/10.1590/1678-4685-gmb-2017-0069.

Fan H *et al.* Chromosome-level genome assembly for giant panda provides novel insights into carnivora chromosome evolution. *Genome Biol*. 2019:20:1–12. https://doi.org/10.1186/s13059-019-1889-7.

Festa-Bianchet M, Apollonio M. *Animal behavior and wildlife conservation*. Island Press; 2003.

Finn RD, Clements J, Eddy SR. HMMER web server: interactive sequence similarity searching. *Nucleic Acids Res*. 2011:39:W29–W37. https://doi.org/10.1093/nar/gkr367.

Fitak RR *et al.* Genomic signatures of domestication in Old World camels. *Commun Biol*. 2020:3:1–10. https://doi.org/10.1038/s42003-020-1039-5.

Formenti G *et al.* Complete vertebrate mitogenomes reveal widespread repeats and gene duplications. *Genome Biol*. 2021:22:1–22. https://doi.org/10.1186/s13059-021-02336-9.

Gabriel L *et al.* BRAKER3: Fully automated genome annotation using RNA-seq and protein evidence with GeneMark-ETP, AUGUSTUS, and TSEBRA. *Genome Res*. 2024:34:769–777. https://doi.org/10.1101/gr.278090.123.

Gabriel L, Hoff KJ, Brůna T, Borodovsky M, Stanke M. TSEBRA: transcript selector for BRAKER. *BMC Bioinformatics*. 2021:22:1–12. https://doi.org/10.1186/s12859-021-04482-0.

Ghurye J, Pop M, Koren S, Bickhart D, Chin C-S. Scaffolding of long read assemblies using long range contact information. *BMC Genomics*. 2017:18:1–11. https://doi.org/10.1186/s12864-017-3879-z.

Glikman JA *et al.* Local attitudes toward Apennine brown bears: insights for conservation issues. *Conserv Sci Pract*. 2019:1:e25. https://doi.org/10.1111/csp2.25.

Glikman JA, Frank B, D'Amico D, Boitani L, Ciucci P. Sharing land with bears: insights toward effective coexistence. *J Nat Conserv*. 2023:74:126421. https://doi.org/10.1016/j.jnc.2023.126421.

Goel M, Schneeberger K. Plotsr: visualizing structural similarities and rearrangements between multiple genomes. *Bioinformatics*. 2022:38:2922–2926. https://doi.org/10.1093/bioinformatics/btac196.

Goel M, Sun H, Jiao W-B, Schneeberger K. SyRI: finding genomic rearrangements and local sequence differences from whole-genome assemblies. *Genome Biol*. 2019:20:1–13. https://doi.org/10.1186/s13059-019-1911-0.

Goes FS *et al.* Genome-wide association of mood-incongruent psychotic bipolar disorder. *Transl Psychiatry*. 2012:2:e180. https://doi.org/10.1038/tp.2012.106.

Grosso AR *et al.* Tissue-specific splicing factor gene expression signatures. *Nucleic Acids Res*. 2008:36:4823–4832. https://doi.org/10.1093/nar/gkn463.

Guan D *et al.* Identifying and removing haplotypic duplication in primary genome assemblies. *Bioinformatics*. 2020:36:2896–2898. https://doi.org/10.1093/bioinformatics/btaa025.

Hao Z *et al. RIdeogram*: drawing SVG graphics to visualize and map genome-wide data on the idiograms. *PeerJ Comput Sci*. 2020:6:e251. https://doi.org/10.7717/peerj-cs.251.

Herbeck YE, Eliava M, Grinevich V, MacLean EL. Fear, love, and the origins of canid domestication: an oxytocin hypothesis. *Compr Psychoneuroendocrinol*. 2022:9:100100. https://doi.org/10.1016/j.cpnec.2021.100100.

Howe K *et al.* Significantly improving the quality of genome assemblies through curation. *Gigascience*. 2021:10:1–9. https://doi.org/10.1093/gigascience/giaa153.

Hulsman Hanna LL *et al.* Genome-wide association study of temperament and tenderness using different Bayesian approaches in a Nellore-Angus crossbred population. *Livest Sci*. 2014:161:17–27. https://doi.org/10.1016/j.livsci.2013.12.012.

Hunter S *et al.* InterPro in 2011: new developments in the family and domain prediction database. *Nucleic Acids Res*. 2012:40:D306–D312. https://doi.org/10.1093/nar/gkr948.

Jaganathan K *et al.* Predicting splicing from primary sequence with deep learning. *Cell*. 2019:176:535–548.e24. https://doi.org/10.1016/j.cell.2018.12.015.

Jeffares DC *et al.* Transient structural variations have strong effects on quantitative traits and reproductive isolation in fission yeast. *Nat Commun*. 2017:8:1–11. https://doi.org/10.1038/ncomms14061.

Jelen N, Ule J, Živin M, Darnell RB. Evolution of Nova-dependent splicing regulation in the brain. *PLoS Genet*. 2007:3:1838–1847. https://doi.org/10.1371/journal.pgen.0030173.

Jennison G. *Animals for show and pleasure in ancient Rome*. Manchester University Press; 1937.

Jiang X, Assis R. Population-specific genetic and expression differentiation in Europeans. *Genome Biol Evol*. 2020:12:358–369. https://doi.org/10.1093/gbe/evaa021.

Kaplan JO *et al.* Holocene carbon emissions as a result of anthropogenic land cover change. *Holocene*. 2011:21:775–791. https://doi.org/10.1177/0959683610386983.

Kardos M *et al.* The crucial role of genome-wide genetic variation in conservation. *Proc Natl Acad Sci U S A*. 2021:118:e2104642118. https://doi.org/10.1073/pnas.2104642118.

Katoh K, Standley DM. MAFFT multiple sequence alignment software version 7: improvements in performance and usability. *Mol Biol Evol*. 2013:30:772–780. https://doi.org/10.1093/molbev/mst010.

Kearse M *et al.* Geneious basic: an integrated and extendable desktop software platform for the organization and analysis of sequence data. *Bioinformatics*. 2012:28:1647–1649. https://doi.org/10.1093/bioinformatics/bts199.

Kim D, Langmead B, Salzberg SL. HISAT: a fast spliced aligner with low memory requirements. *Nat Methods*. 2015:12:357–360. https://doi.org/10.1038/nmeth.3317.

Kolberg L *et al.* G:profiler—interoperable web service for functional enrichment analysis and gene identifier mapping (2023 update). *Nucleic Acids Res*. 2023:51:W207–W212. https://doi.org/10.1093/nar/gkad347.

Kuhl H *et al.* CSA: a high-throughput chromosome-scale assembly pipeline for vertebrate genomes. *Gigascience*. 2020:9:1–14. https://doi.org/10.1093/gigascience/giaa034.

Kuznetsov D *et al.* OrthoDB v11: annotation of orthologs in the widest sampling of organismal diversity. *Nucleic Acids Res*. 2023:51:D445–D451. https://doi.org/10.1093/nar/gkac998.

Laidre KL *et al.* Glacial ice supports a distinct and undocumented polar bear subpopulation persisting in late 21st-century sea-ice conditions. *Science*. 2022:376:1333–1338. https://doi.org/10.1126/science.abk2793.

Layer RM, Chiang C, Quinlan AR, Hall IM. LUMPY: a probabilistic framework for structural variant discovery. *Genome Biol*. 2014:15:1–19. https://doi.org/10.1186/gb-2014-15-6-r84.

Levis NA, Pfennig DW. Plasticity-led evolution: a survey of developmental mechanisms and empirical tests. *Evol Dev*. 2020:22:71–87. https://doi.org/10.1111/ede.12309.

Lewis MA *et al.* Learning and animal movement. *Front Ecol Evol*. 2021:9:681704. https://doi.org/10.3389/fevo.2021.681704.

Li H *et al.* The sequence alignment/map format and SAMtools. *Bioinformatics*. 2009:25:2078–2079. https://doi.org/10.1093/bioinformatics/btp352.

Li H. A statistical framework for SNP calling, mutation discovery, association mapping and population genetical parameter estimation from sequencing data. *Bioinformatics*. 2011:27:2987–2993. https://doi.org/10.1093/bioinformatics/btr509.

Li H. Minimap2: pairwise alignment for nucleotide sequences. *Bioinformatics*. 2018:34:3094–3100. https://doi.org/10.1093/bioinformatics/bty191.

Li H, Durbin R. Inference of human population history from individual whole-genome sequences. *Nature*. 2011:475:493–496. https://doi.org/10.1038/nature10231.

Liang YT, Luo H, Lin Y, Gao F. Recent advances in the characterization of essential genes and development of a database of essential genes. *iMeta*. 2024:3:e157. https://doi.org/10.1002/imt2.157.

Liu S *et al.* Population genomics reveal recent speciation and rapid evolutionary adaptation in polar bears. *Cell*. 2014:157:785–794. https://doi.org/10.1016/j.cell.2014.03.054.

Loy A, Genov P, Galfo M, Jacobone MG, Taglianti AV. Cranial morphometrics of the Apennine brown bear (*Ursus arctos marsicanus*) and preliminary notes on the relationships with other southern European populations. *Ital J Zool*. 2008:75:67–75. https://doi.org/10.1080/11250000701689857.

Mancinelli S, Falco M, Boitani L, Ciucci P. Social, behavioural and temporal components of wolf (*Canis lupus*) responses to anthropogenic landscape features in the central Apennines, Italy. *J Zool*. 2019:309:114–124. https://doi.org/10.1111/jzo.12708.

Manni M, Berkeley MR, Seppey M, Simão FA, Zdobnov EM. BUSCO update: novel and streamlined workflows along with broader and deeper phylogenetic coverage for scoring of eukaryotic, prokaryotic, and viral genomes. *Mol Biol Evol*. 2021:38:4647–4654. https://doi.org/10.1093/molbev/msab199.

Mapleson D, Venturini L, Kaithakottil G, Swarbreck D. Efficient and accurate detection of splice junctions from RNA-Seq with portcullis. *Gigascience*. 2018:7:1–11. https://doi.org/10.1093/gigascience/giy131.

Marlon JR *et al.* Global biomass burning: a synthesis and review of Holocene paleofire records and their controls. *Quat Sci Rev*. 2013:65:5–25. https://doi.org/10.1016/j.quascirev.2012.11.029.

Maroso F *et al.* Fitness consequences and ancestry loss in the Apennine brown bear after a simulated genetic rescue intervention. *Conserv Biol*. 2023:37. https://doi.org/10.1111/cobi.14133.

Martínez-Abraín A *et al.* Ecological consequences of human depopulation of rural areas on wildlife: a unifying perspective. *Biol Conserv*. 2020:252:108860. https://doi.org/10.1016/j.biocon.2020.108860.
Martínez-Abraín A, Jiménez J, Oro D. Pax Romana: "refuge abandonment" and spread of fearless behavior in a reconciling world. *Anim Conserv*. 2019:22:3–13. https://doi.org/10.1111/acv.12429.
Martínez-Abraín A, Quevedo M, Serrano D. Translocation in relict shy-selected animal populations: program success versus prevention of wildlife-human conflict. *Biol Conserv*. 2022:268:109519. https://doi.org/10.1016/j.biocon.2022.109519.
McDougall PT, Réale D, Sol D, Reader SM. Wildlife conservation and animal temperament: causes and consequences of evolutionary change for captive, reintroduced, and wild populations. *Anim Conserv*. 2006:9:39–48. https://doi.org/10.1111/j.1469-1795.2005.00004.x.
McKenna A *et al.* The genome analysis toolkit: a MapReduce framework for analyzing next-generation DNA sequencing data. *Genome Res*. 2010:20:1297–1303. https://doi.org/10.1101/gr.107524.110.
Mead D *et al.* The genome sequence of the Eurasian river otter, *Lutra lutra* Linnaeus 1758. *Wellcome Open Res*. 2020:5:33. https://doi.org/10.12688/wellcomeopenres.15722.1.
Meloro C, Guidarelli G, Colangelo P, Ciucci P, Loy A. Mandible size and shape in extant Ursidae (Carnivora, Mammalia): a tool for taxonomy and ecogeography. *J Zool Syst Evol Res*. 2017:55:269–287. https://doi.org/10.1111/jzs.12171.
Merilä J, Hendry AP. Climate change, adaptation, and phenotypic plasticity: the problem and the evidence. *Evol Appl*. 2014:7:1–14. https://doi.org/10.1111/eva.12137.
Miller W *et al.* Polar and brown bear genomes reveal ancient admixture and demographic footprints of past climate change. *Proc Natl Acad Sci U S A*. 2012:109:E2382–E2390. https://doi.org/10.1073/pnas.1210506109.
Mohr DW *et al.* A chromosome-length assembly of the Hawaiian monk seal (*Neomonachus schauinslandi*): a history of "genetic purging" and genomic stability. *Genes (Basel)*. 2022:13:1270. https://doi.org/10.3390/genes13071270.
Montague MJ *et al.* Comparative analysis of the domestic cat genome reveals genetic signatures underlying feline biology and domestication. *Proc Natl Acad Sci U S A*. 2014:111:17230–17235. https://doi.org/10.1073/pnas.1410083111.
Mueller JC, Partecke J, Hatchwell BJ, Gaston KJ, Evans KL. Candidate gene polymorphisms for behavioural adaptations during urbanization in blackbirds. *Mol Ecol*. 2013:22:3629–3637. https://doi.org/10.1111/mec.12288.
Nadachowska-Brzyska K *et al.* Genomic inference of contemporary effective population size in a large island population of collared flycatchers (*Ficedula albicollis*). *Mol Ecol*. 2021:30:3965–3973. https://doi.org/10.1111/mec.16025.
Nash WG, O'Brien SJ. A comparative chromosome banding analysis of the Ursidae and their relationship to other carnivores. *Cytogenet Cell Genet*. 1987:45:206–212. https://doi.org/10.1159/000132455.
Novo I *et al.* Impact of population structure in the estimation of recent historical effective population size by the software GONE. *Genet Sel Evol*. 2023:55:1–15. https://doi.org/10.1186/s12711-023-00859-2.
Oriol-Cotterill A, Valeix M, Frank LG, Riginos C, Macdonald DW. Landscapes of coexistence for terrestrial carnivores: the ecological consequences of being downgraded from ultimate to penultimate predator by humans. *Oikos*. 2015:124:1263–1273. https://doi.org/10.1111/oik.02224.
O'Rourke T, Boeckx C. Glutamate receptors in domestication and modern human evolution. *Neurosci Biobehav Rev*. 2020:108:341–357. https://doi.org/10.1016/j.neubiorev.2019.10.004.
Ortega-Campos SM, García-Heredia JM. The multitasker protein: a look at the multiple capabilities of NUMB. *Cells*. 2023:12:333. https://doi.org/10.3390/cells12020333.
Otto SP. Adaptation, speciation and extinction in the Anthropocene. *Proc R Soc B Biol Sci*. 2018:285:20182047. https://doi.org/10.1098/rspb.2018.2047.
Ou S *et al.* Benchmarking transposable element annotation methods for creation of a streamlined, comprehensive pipeline. *Genome Biol*. 2019:20:1–18. https://doi.org/10.1186/s13059-019-1905-y.
Palumbi SR. Humans as the world's greatest evolutionary force. *Science*. 2001:293:1786–1790. https://doi.org/10.1126/science.293.5536.1786.
Paradis E, Schliep K. Ape 5.0: an environment for modern phylogenetics and evolutionary analyses in R. *Bioinformatics*. 2019:35:526–528. https://doi.org/10.1093/bioinformatics/bty633.
Parikh H *et al.* Svclassify: a method to establish benchmark structural variant calls. *BMC Genomics*. 2016:17:1–16. https://doi.org/10.1186/s12864-016-2366-2.
Park E, Pan Z, Zhang Z, Lin L, Xing Y. The expanding landscape of alternative splicing variation in human populations. *Am J Hum Genet*. 2018:102:11–26. https://doi.org/10.1016/j.ajhg.2017.11.002.
Pelletier F, Coltman DW. Will human influences on evolutionary dynamics in the wild pervade the Anthropocene? *BMC Biol*. 2018:16:7. https://doi.org/10.1186/s12915-017-0476-1.
Pendleton AL *et al.* Comparison of village dog and wolf genomes highlights the role of the neural crest in dog domestication. *BMC Biol*. 2018:16:1–21. https://doi.org/10.1186/s12915-018-0535-2.
Peng Y *et al.* Down-regulation of *EPAS1* transcription and genetic adaptation of Tibetans to high-altitude hypoxia. *Mol Biol Evol*. 2017:34:818–830. https://doi.org/10.1093/molbev/msw280.
Penteriani V *et al.* Human behaviour can trigger large carnivore attacks in developed countries. *Sci Rep*. 2016:6:1–8. https://doi.org/10.1038/srep20552.
Piva F, Giulietti M, Burini AB, Principato G. SpliceAid 2: a database of human splicing factors expression data and RNA target motifs. *Hum Mutat*. 2012:33:81–85. https://doi.org/10.1002/humu.21609.
Plagnol V *et al.* A robust model for read count data in exome sequencing experiments and implications for copy number variant calling. *Bioinformatics*. 2012:28:2747–2754. https://doi.org/10.1093/bioinformatics/bts526.
Punta M *et al.* The Pfam protein families database. *Nucleic Acids Res*. 2012:40:D290–D301. https://doi.org/10.1093/nar/gkr1065.
Purcell S *et al.* PLINK: a tool set for whole-genome association and population-based linkage analyses. *Am J Hum Genet*. 2007:81:559–575. https://doi.org/10.1086/519795.
Quevillon E *et al.* InterProScan: protein domains identifier. *Nucleic Acids Res*. 2005:33:W116–W120. https://doi.org/10.1093/nar/gki442.
Quinlan AR, Hall IM. BEDTools: a flexible suite of utilities for comparing genomic features. *Bioinformatics*. 2010:26:841–842. https://doi.org/10.1093/bioinformatics/btq033.
Raponi M *et al.* Prediction of single-nucleotide substitutions that result in exon skipping: identification of a splicing silencer in *BRCA1* exon 6. *Hum Mutat*. 2011:32:436–444. https://doi.org/10.1002/humu.21458.
Rausch T *et al.* DELLY: structural variant discovery by integrated paired-end and split-read analysis. *Bioinformatics*. 2012:28:i333–i339. https://doi.org/10.1093/bioinformatics/bts378.
Renaud G, Hanghøj K, Korneliussen TS, Willerslev E, Orlando L. Joint estimates of heterozygosity and runs of homozygosity for modern and ancient samples. *Genetics*. 2019:212:587–614. https://doi.org/10.1534/genetics.119.302057.
Riepe TV, Khan M, Roosing S, Cremers FPM, 't Hoen PAC. Benchmarking deep learning splice prediction tools using functional splice assays. *Hum Mutat*. 2021:42:799–810. https://doi.org/10.1002/humu.24212.
Rigby MJ *et al.* SLC13A5/sodium-citrate co-transporter overexpression causes disrupted white matter integrity and an autistic-like phenotype. *Brain Commun*. 2022:4:fcac002. https://doi.org/10.1093/braincomms/fcac002.
Ripple WJ *et al.* Status and ecological effects of the world's largest carnivores. *Science*. 2014:343:1241484. https://doi.org/10.1126/science.1241484.
Saito Y *et al.* NOVA2-mediated RNA regulation is required for axonal pathfinding during development. *Elife*. 2016:5:e14371. https://doi.org/10.7554/eLife.14371.

Santiago E *et al.* Recent demographic history inferred by high-resolution analysis of linkage disequilibrium. *Mol Biol Evol*. 2020:37:3642–3653. https://doi.org/10.1093/molbev/msaa169.

Schell CJ *et al.* The evolutionary consequences of human–wildlife conflict in cities. *Evol Appl*. 2021:14:178–197. https://doi.org/10.1111/eva.13131.

Schubert C. The genomic basis of the Williams–Beuren syndrome. *Cell Mol Life Sci*. 2009:66:1178–1197. https://doi.org/10.1007/s00018-008-8401-y.

Schubert M *et al.* Prehistoric genomes reveal the genetic foundation and cost of horse domestication. *Proc Natl Acad Sci U S A*. 2014:111:E5661–E5669. https://doi.org/10.1073/pnas.1416991111.

Schubert M, Lindgreen S, Orlando L. AdapterRemoval v2: rapid adapter trimming, identification, and read merging. *BMC Res Notes*. 2016:9:1–7. https://doi.org/10.1186/s13104-016-1900-2.

Selch S *et al.* Analysis of naturally occurring mutations in the human uptake transporter NaCT important for bone and brain development and energy metabolism. *Sci Rep*. 2018:8:11330. https://doi.org/10.1038/s41598-018-29547-8.

Sih A, Bell A, Johnson JC. Behavioral syndromes: an ecological and evolutionary overview. *Trends Ecol Evol*. 2004:19:372–378. https://doi.org/10.1016/j.tree.2004.04.009.

Smit A, Hubley R, Green P. RepeatMasker Open-4.0. 2013. http://repeatmasker.org.

Srivastava A *et al.* Genome assembly and gene expression in the American black bear provides new insights into the renal response to hibernation. *DNA Res*. 2019:26:37–44. https://doi.org/10.1093/dnares/dsy036.

Stamatakis A. RAxML version 8: a tool for phylogenetic analysis and post-analysis of large phylogenies. *Bioinformatics*. 2014:30:1312–1313. https://doi.org/10.1093/bioinformatics/btu033.

Stanke M *et al.* AUGUSTUS: a b initio prediction of alternative transcripts. *Nucleic Acids Res*. 2006:34:W435–W439. https://doi.org/10.1093/nar/gkl200.

Stanyon R, Galleni L. A rapid fibroblast culture technique for high resolution karyotypes. *Bolletino di Zool*. 1991:58:81–83. https://doi.org/10.1080/11250009109355732.

Štofík J, Bučko J, Gič M, Saniga M. Time and spatial trends in the brown bear *Ursus arctos* population in Slovakia (1900–2010). *Folia Oecologica*. 2013:40:117–129.

Stuart KC, Edwards RJ, Sherwin WB, Rollins LA. Contrasting patterns of single nucleotide polymorphisms and structural variation across multiple invasions. *Mol Biol Evol*. 2023:40:msad046. https://doi.org/10.1093/molbev/msad046.

Supple MA *et al.* A genome assembly of the American black bear, *Ursus americanus*, from California. *J Hered*. 2024:115:498–506. https://doi.org/10.1093/jhered/esae037.

Szklarczyk D *et al.* The STRING database in 2023: protein-protein association networks and functional enrichment analyses for any sequenced genome of interest. *Nucleic Acids Res*. 2023:51:D638–D646. https://doi.org/10.1093/nar/gkac1000.

Taylor GA *et al.* The genome of the North American brown bear or grizzly: *Ursus arctos* ssp. Horribilis. *Genes (Basel)*. 2018:9:598. https://doi.org/10.3390/genes9120598.

Tenan S *et al.* Evaluating mortality rates with a novel integrated framework for nonmonogamous species. *Conserv Biol*. 2016:30:1307–1319. https://doi.org/10.1111/cobi.12736.

Theofanopoulou C *et al.* Self-domestication in *Homo sapiens*: insights from comparative genomics. *PLoS One*. 2017:12:e0185306. https://doi.org/10.1371/journal.pone.0185306.

Thompson EA. Identity by descent: variation in meiosis, across genomes, and in populations. *Genetics*. 2013:194:301–326. https://doi.org/10.1534/genetics.112.148825.

Thompson R. *No word for wilderness: Italy's Grizzlies and the race to save the rarest bears on earth*. Ashland Creek Press; 2018.

Trut LN. Early canid domestication: the farm-fox experiment: foxes bred for tamability in a 40-year experiment exhibit remarkable transformations that suggest an interplay between behavioral genetics and development. *Am Sci*. 1999:87:160–169. https://doi.org/10.1511/1999.20.160.

Tuomainen U, Candolin U. Behavioural responses to human-induced environmental change. *Biol Rev Camb Philos Soc*. 2011:86:640–657. https://doi.org/10.1111/j.1469-185X.2010.00164.x.

VonHoldt BM *et al.* Structural variants in genes associated with human Williams–Beuren syndrome underlie stereotypical hypersociability in domestic dogs. *Sci Adv*. 2017:3:e1700398. https://doi.org/10.1126/sciadv.1700398.

Wang G-D *et al.* Out of southern east Asia: the natural history of domestic dogs across the world. *Cell Res*. 2016:26:21–33. https://doi.org/10.1038/cr.2015.147.

Wang X *et al.* Genomic responses to selection for tame/aggressive behaviors in the silver fox (*Vulpes vulpes*). *Proc Natl Acad Sci U S A*. 2018:115:10398–10403. https://doi.org/10.1073/pnas.1800889115.

Whittaker D, Knight RL. Understanding wildlife responses to humans. *Wildl Soc Bull*. 1998:26:312–317.

Xu M *et al.* TGS-GapCloser: a fast and accurate gap closer for large genomes with low coverage of error-prone long reads. *Gigascience*. 2020:9:giaa094. https://doi.org/10.1093/gigascience/giaa094.

Yan H, Bombarely A, Li S. DeepTE: a computational method for *de novo* classification of transposons with convolutional neural network. *Bioinformatics*. 2020:36:4269–4275. https://doi.org/10.1093/bioinformatics/btaa519.

Yi X *et al.* Sequencing of 50 human exomes reveals adaptation to high altitude. *Science*. 2010:329:75–78. https://doi.org/10.1126/science.1190371.

Zarate S *et al.* Parliament2: accurate structural variant calling at scale. *Gigascience*. 2021:9:1–9. https://doi.org/10.1093/gigascience/giaa145

Zennaro P *et al.* Europe on fire three thousand years ago: arson or climate?. *Geophys Res Lett*. 2015:42:5023–5033. https://doi.org/10.1002/2015GL064259.

Zhou R *et al.* The Meishan pig genome reveals structural variation-mediated gene expression and phenotypic divergence underlying Asian pig domestication. *Mol Ecol Resour*. 2021:21:2077–2092. https://doi.org/10.1111/1755-0998.13396.

Zhu C *et al.* Draft genome assembly for the Tibetan black bear (*Ursus thibetanus thibetanus*). *Front Genet*. 2020:11:231. https://doi.org/10.3389/fgene.2020.00231.

Zimin AV, Salzberg SL. The genome polishing tool POLCA makes fast and accurate corrections in genome assemblies. *PLoS Comput Biol*. 2020:16:e1007981. https://doi.org/10.1371/journal.pcbi.1007981.